THESIS FOR THE DEGREE OF DOCTOR OF PHILOSOPHY

On quantifying the installation effects of displacement piles in natural clays

JONATAN ISAKSSON

Department of Architecture and Civil Engineering

Division of Geology and Geotechnics

CHALMERS UNIVERSITY OF TECHNOLOGY

Gothenburg, Sweden 2025

On quantifying the installation effects of displacement piles in natural clays
JONATAN ISAKSSON
ISBN 978-91-8103-167-6

Doktorsavhandlingar vid Chalmers tekniska högskola
Ny serie nr. 5625
ISSN 0346-718X
Department of Architecture and Civil Engineering
Division of Geology and Geotechnics
Chalmers University of Technology
SE-412 96 Gothenburg
Sweden
Telephone: +46 (0)31-772 1000

Chalmers Digitaltryck
Gothenburg, Sweden 2025

On quantifying the installation effects of displacement piles in natural clays
Thesis for the degree of Doctor of Philosophy
JONATAN ISAKSSON
Department of Architecture and Civil Engineering
Division of Geology and Geotechnics
Chalmers University of Technology

ABSTRACT

Urbanisation calls for a more efficient use of space. Historically, cities are often located close to water where deep deposits of soft natural clay are ubiquitous. This combination of factors results in construction of increasingly larger buildings on less competent ground, which requires deep foundations. Displacement piles offer one of the most cost-effective deep foundation solutions. The installation of those piles, however, leads to mass-displacements and changes in state in the clay that surrounds the newly built and existing structures in the geotechnical system. Nowadays advanced numerical analysis is routinely used by practising geotechnical engineers to quantify the soil-structure interactions in urban areas. Including the pile installation phase in such system-level analyses, however, is complex and thus often neglected. In practice, designers rely on empirical relations to consider the influence of the installation on the pile response, and the impact of mass-displacement is investigated as a separate design case in which the change of state is not considered.

This thesis explores the possibility of directly including pile installation in the numerical analysis of the urban geotechnical system. The focus was on modelling the changes of the soil in space and time during (parts of) the pile cycle using numerical techniques. The research results show that the pile installation phase can be successfully modelled at each stage of the pile cycle, using realistic kinematics by using a numerical framework for large deformations and a constitutive model that captures the complex deformation characteristics of soft natural clays. Furthermore, the need for complexity in the numerical analysis, in terms of modelling the kinematics of pile installation and the constitutive model, was investigated. Geotechnical engineers should avoid using advanced constitutive models while neglecting the influence of pile installation. The simplified models perform well in comparison to the advanced models for predicting the short-term response at distances larger than five pile radii. The results reiterate that short-term mass-displacements occur in undrained conditions and that the length and cross-sectional area, in combination with the relation between the pile length and distance from the pile, govern the distribution of soil displacements. Additionally, stiff boundaries, existing foundations, as well as horizontal and vertical stiffness gradients influenced the distribution of the displaced soil. In conclusion, the work conducted in this thesis provides a basis for further numerical studies on the influence of pile installation on the urban geotechnical systems.

Keywords: deep foundations, pile installation, mass-displacements, numerical modelling, soft natural clay, soil-structure interaction, Creep-SCLAY1S

ACKNOWLEDGEMENTS

This work has been financially supported by the Development Fund of the Swedish Construction Industry (SBUF) by grants 13614 and 14186, the Swedish Transport Administration (Trafikverket) via the research programme BIG (Branschsamverkan i grunden) by grants A2019-19 and B2019-19, and by NCC AB. The financial support is gratefully acknowledged. Furthermore, I would like to express my deep and humble gratitude to society for the opportunity to spend 26 years in the public education system.

I want to thank my main supervisor, Prof. Jelke Dijkstra, for the discussions, the laughter, your curiosity and kindness, and your aid in getting things done. To the seniors in the Geotechnics group, my co-supervisor Mats Karlsson, my examiner Minna Karstunen and Ayman Abed, I am grateful for your open doors, warm hearts and willingness to share your experience and knowledge. To all former and current colleagues at Chalmers, I am thankful for all the discussions, your helpfulness, and, foremost, for our everyday friendship.

To my colleagues at NCC Teknik, thank you for checking in and making me feel like part of the group during my five-year absence, and reminding me that there is something else to work-life besides Chalmers. Thanks to my industry supervisors, Jorge Yannie and Lars Hall for your support. To my colleagues at NCC R&I, I am glad to have spent my PhD journey with you and I am thankful for your perspectives and passion to perform.

To my family, thank you for sharing my joy of knowledge and for forming me into who I am today. Amanda, thank you for every day together, for your encouragement and support; well done to us for getting through the fall/winter 2024-2025 together! Ines, thank you for helping me focus on the essential things in life during my last year of PhD studies.

Jonatan Isaksson
Göteborg, 2025

List of publications

This thesis consists of an extended summary and the following appended papers:

Paper A Isaksson, J., Yannie, J., Karlsson, M., & Dijkstra, J. (2022). Simulation of CPT penetration in sensitive clay. In Gottardi & Tonni (Eds.), *Proceedings of the 5th International Symposium on Cone Penetration Testing, CPT 2022* (pp. 480–485). CRC Press. https://doi.org/10.1201/9781003308829-67

Paper B Isaksson, J., Karlsson, M., & Dijkstra, J. (2023). Modelling pile installation in soft natural clays. L. Zdravkovic, S. Kontoe, T. DMG, & T. A. (Eds.), *Proceedings 10th European Conference on Numerical Methods in Geotechnical Engineering*. https://doi.org/10.53243/NUMGE2023-48

Paper C Isaksson, J., & Dijkstra, J. (Forthcoming). Modeling the pile cycle of an axially loaded pile in sensitive natural clay. *Journal of Geotechnical and Geoenvironmental Engineering*. https://doi.org/10.1061/JGGEFK/GTENG-13179

Paper D Isaksson, J., Tahershamsi, H., & Dijkstra, J. (2025b). On modelling pile installation in soft natural clay. *Submitted manuscript*

Paper E Isaksson, J., Li, Y., & Hall, L. (2024). A simple method for predicting cohesive pile deformations from displacement pile installation induced ground movement. *19th Nordic Geotechnical Meeting, Gothenburg*

Paper F Isaksson, J., Karlsson, M., & Dijkstra, J. (2025a). Quantifying the response of piled structures from displacements induced by pile installation in soft clay. *Canadian Geotechnical Journal,* [Preprint]. https://doi.org/10.1139/cgj-2024-0387

OTHER RELATED PUBLICATIONS

- Wong, D. Y. C., Sadasivan, V., Isaksson, J., Karlsson, A., & Dijkstra, J. (2024). Trans-scale spatial variability of lime-cement mixed columns. *Construction and Building Materials*, *417*. https://doi.org/10.1016/j.conbuildmat.2024.135394

TABLE OF CONTENTS

NOTATION

Acronyms

CPTU	piezocone penetration test
CRS	Constant Rate of Strain
CS	Critical State
CSL	Critical State Line
NCL	Normal Compression Line
OCR	Apparent Overconsolidation ratio
SSPM	Shallow Strain Path Method

Greek symbols

α	amount of anisotropy
α_s	adhesion factor at pile failure
β	effective stress factor at pile failure
γ	unit weight
Δu	excess pore pressure
δ	displacement
$\dot{\varepsilon}$	strain rate
ε	strain
κ	swelling index
κ^*	modified swelling index
λ	compression index
λ^*	modified compression index
λ_{i}	intrinsic compression index
λ_{i}^*	modified intrinsic compression index
μ^*	modified intrinsic creep index
ν'	Poisson's ratio
ϖ	small strain multiplier
ρ	density
σ'_{h}	horizontal effective stress
σ'_{v}	vertical effective stress
σ'_h	horizontal effective stress
σ'_r	radial effective stress
σ'_{vc}	apparent vertical preconsolidation pressure
τ_f	shaft resistance at failure
χ	amount of bonding
Ω	installed pile volume
ω	rate of rotational hardening
ω_{d}	relative rate of rotational hardening due to deviatoric strain

Roman lower case letters

a	rate of destructuration
b	relative rate of destructuration due to deviatoric strain
c_{h}	horizontal coefficient of consolidation
c_{v}	vertical coefficient of consolidation
d	diameter
e	void ratio
k	permeability (hydraulic conductivity)
p'	mean effective stress
q	deviatoric stress
q_p	penetrometer resistance
q_{net}	CPTU net tip resistance
s_{u}	undrained shear strength
t	time
u	pore pressure
v	penetration velocity
w_L	water content at liquid limit
w_n	natural water content
w_p	water content at plastic limit

Roman capital letters

A	shape factor for small strain stiffness degradation
E	Young's modulus
G	shear modulus
I_p	plasticity index
K'	effective bulk modulus
K_0	coefficient of earth pressure at rest
K_c	coefficient of earth pressure after equalisation
K_i	coefficient of earth pressure after installation
L	pile length
M_{c}	stress ratio at critical state in triaxial compression
M_{e}	stress ratio at critical state in triaxial extension
R	radius
S_t	sensitivity
T	normalised time (time factor)
V	normalised penetration velocity

Part I
Extended summary

1 Introduction

1.1 Background

Historically, human settlements have been established near lakes, rivers and other waterways often situated on deep deposits of soft natural clay. Some of these early settlements have transformed into the cities of today, comprising of modern structures that have been built adjacent to existing (historic) structures. Furthermore, building plots have been re-used, leading to new developments in the same location as demolished structures. Urbanisation calls for increasingly more efficient use of the urban space, leading to the construction of high-rise buildings and increasingly higher loads on new foundations. In addition to securing the bearing capacity and controlling the deformations of the new foundation, predicting the influence of the new building on the neighbouring structures and their foundations has become an essential part of the foundation design in urban settings. Furthermore, the contribution of the construction sector to global warming is significant and an efficient use of construction materials, including those in the foundation, is essential in the effort towards net zero emissions (De Melo et al. 2024).

A system perspective is required to predict the spatio-temporal response of the complex urban geotechnical systems. The response of these systems is a result of the interactions between the soil in its current state, including the existing structures, and the changes to the system caused by the new structures. Deep foundations are used to transfer large loads from the super-structure to the clay deposit below and are thus a common component in the urban geotechnical system. The installation of piles will impact the system by a combination of state change and mass displacements (*e.g.*, Bozozuk et al. 1978). In Sweden, driven prefabricated concrete displacement piles comprise *ca.* 50–60% of the yearly installed pile volume (Pålkommissionen 2024). During installation, these piles displace the soil with a combination of translation & rotation and deformation (strain), *e.g.*, Ni et al. (2010).

In geotechnical engineering practice, numerical modelling is increasingly more common for analysing geotechnical engineering problems in an urban setting involving soil-structure interaction at system-level. Advanced constitutive models combined with coupled hydro-mechanical Finite Element frameworks have been successfully used to quantify the evolving state of soft natural clays due to historical, present and future loading events. When combined with field- and laboratory-based site investigation methods, numerical modelling gives the geotechnical engineer a powerful tool to increase the understanding and to quantify the current and future state of the system (*e.g.* Zdravković et al. 2021; Karstunen 2023).

Including the effects of pile installation in geotechnical system analysis, however, is complex and thus usually simplified. The numerical complexity of the pile installation process, resulting from the large deformations around the advancing pile base, precludes the adoption of system-level analyses using standard (small strain) Finite Element formulations.

In current practice, the effect of the pile installation in natural clay is usually included indirectly. Empirical relations between pile load tests and the *in-situ* conditions prior to installation, such as the undrained shear strength, vertical effective stress or cone resistance are most often used for design of the bearing capacity of single piles (or piles at a sufficiently large centre-to-centre spacing). However, the influence of the evolving state of the soil following pile installation on the

larger geotechnical system is often overlooked. In Swedish geotechnical engineering practice, the immediate impact of pile installation is commonly included in the analysis as a separate design case. Typically, only the undrained response in the clay is simulated using the Shallow Strain Path Method (Sagaseta et al. 1997) or simple Finite Element Methods. In contrast, the deformation analysis during the service life of the foundation is often conducted without consideration of the time-dependent effects from pile installation.

A multitude of numerical frameworks are available to address the complexity involved in the modelling of the pile installation process into clay (*e.g.*, van den Berg et al. 1996; Lu et al. 2004; Dijkstra et al. 2011; Hamann et al. 2015; Ceccato et al. 2016; Monforte et al. 2018; Singh et al. 2021; Phek et al. 2023; Staubach et al. 2023). Numerical studies that incorporate the complete service life of the pile, including the installation, with advanced constitutive models in a coupled hydro-mechanical framework, however, remain scarce. Most studies are restricted to the installation of a single pile in an axisymmetric domain without the presence of adjacent structures. Consequently, the influence of pile installation and equalisation on a more complex geotechnical system remains challenging, due to the numerical complexity and the computational demands. Furthermore, the modelling of natural sensitive clays, abundant in the Nordic countries, requires constitutive models that are more advanced than typically used for the modelling of pile installation.

The current project was initiated to investigate potential methods of including the spatio-temporal effects of the installation of displacement piles and subsequent equalisation in geotechnical system analysis. Installation effects will be studied, over the service life of the pile, with a focus on possible means of increasing the accuracy of numerical predictions of the urban geotechnical system. Gothenburg, Sweden, is a typical example of a city that forms such a geotechnical system. The city is situated on a deep deposit, *i.e.*, up to 80 m of soft natural clay and is in the process of densifying the central parts, which requires extensive piling works in an already crowded urban environment.

Different modelling approaches are associated with varying levels of complexity, which apply to both the effort needed by the engineer to use the model and the accuracy of the numerical results obtained. The research will provide guidance on the appropriate model choice for the trade-off between model complexity and the fidelity of the results obtained.

1.2 The pile cycle

In this work, the pile cycle, as proposed by Randolph and Gourvenec (2011), will be used as a conceptual model for the systematic analysis of the spatio-temporal influence of pile installation on the geotechnical system. The pile cycle contains four separate stages and is illustrated in Figure 1.1.

The *in-situ* stage focuses on the state of the soil at the site prior to the installation of the pile. The *installation* of the pile will result in severe distortion in the soil surrounding the pile, leading to a change in the stress distribution and state of the soil. The new effective stress state in the soil after pile installation is a combination of the total stresses in the soil and the changes in the pore water pressures. During the *equalisation* stage, the excess pore water pressures generated during installation dissipate, resulting in an increase in effective stress and a decrease in the total stress

close to the pile. The final stage is the *loading* of the pile, in which the service load is applied to the pile head and transferred to the soil surrounding the pile.

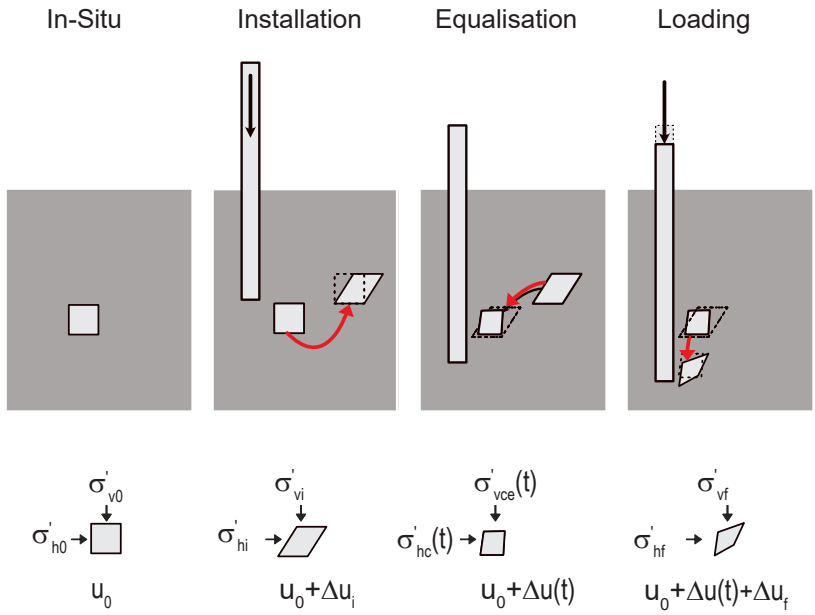

Figure 1.1: *The pile cycle. Separation of the service life of a pile into four different stages. Adopted from Randolph and Gourvenec (2011).*

1.3 Aim and objectives

The spatio-temporal response of the geotechnical system, *i.e.*, the evolving interaction between existing and new structural elements and the soil over time, will be numerically quantified for the installation of displacement piles into soft natural clays. The applicability of the methods with varying degrees of complexity will be studied for several aspects of the pile installation problem, *e.g.*, mass-displacements, evolving state in the soil and the impact on existing foundations.

The main objectives are to investigate:

(i) The influence of model complexity, *i.e.*, numerical framework and constitutive model, on the magnitude of the predicted mass displacements from pile installation in a soft natural clay, including both the short- and long-term conditions.

(ii) The evolving response with time of the state of the pile-soil system over the course of the pile cycle.

(iii) The impact of existing structures and the size of the domain on the distribution of constant volume mass-displacements due to pile installation.

2 Deformation characteristics of soft natural clays

The response of saturated soft natural clay as an engineering material results from its constituents (clay mineralogy and other non-active fractions), geological and anthropogenic deposition and loading history as well as loading conditions (direction, rate). At a continuum level, this evolving mechanical behaviour shows features such as; rate-dependency, anisotropic yielding and stress-strain response as well as strain-softening from destructuration (loss of bonding). This Chapter will briefly discuss some of the main features of the behaviour of soft natural (sensitive) clays, which are needed to understand the response of the pile-soil system over the different stages of the pile cycle. Additionally, a generalised framework will be introduced for numerical studies on the effect of the installation of displacement piles in natural clay.

2.1 Stiffness

Stiffness is a measure of the resistance of a soil to deformations when subjected to a change in stress. In the following, the initial focus is on the effective stress response, *i.e.*, the resistance of the soil skeleton to a change in effective stress. The undrained response, where the water contributes to the bulk stiffness of the soils with a low hydraulic conductivity, will be treated as a special case. For soft natural clays, the link between the emerging continuum response and the mechanisms at particle scale between individual particles is still unresolved (*e.g.*, Birmpilis et al. 2022). The emerging stiffness at continuum scale, however, is well established for monotonic loading paths.

The deformations of a soil element are commonly separated into compression, *i.e.*, a change in volume with a constant shape, and distortion, *i.e.*, a change in shape under constant volume. Correspondingly, the conjugate effective stress components, *i.e.*, the stress component that induces compression and the component that induces distortion can be derived from the the Cauchy stress tensor:

$$\boldsymbol{\sigma'} = \begin{bmatrix} \sigma_x^{'} & \sigma_y^{'} & \sigma_z^{'} & \tau_{xy} & \tau_{yz} & \tau_{zx} \end{bmatrix}^T \tag{2.1}$$

with the following corresponding strain tensor:

$$\boldsymbol{\varepsilon} = \begin{bmatrix} \varepsilon_x & \varepsilon_y & \varepsilon_z & \varepsilon_{xy} & \varepsilon_{yz} & \varepsilon_{zx} \end{bmatrix}^T \tag{2.2}$$

The deviatoric stress tensor and strain tensor can be derived by introducing the isotropic effective stress (also denoted mean effective stress) $p' = (\sigma'_x + \sigma'_y + \sigma'_z)/3$ and volumetric strain $\varepsilon_v = \varepsilon_x + \varepsilon_y + \varepsilon_z$. The deviatoric stress tensor now becomes:

$$\boldsymbol{\sigma'}_d = \begin{bmatrix} \sigma'_x - p' & \sigma'_y - p' & \sigma'_z - p' & \sqrt{2}\tau_{xy}^{'} & \sqrt{2}\tau_{yz}^{'} & \sqrt{2}\tau_{zx}^{'} \end{bmatrix}^T \tag{2.3}$$

and the corresponding deviatoric strain tensor:

$$\boldsymbol{\varepsilon}_d = \begin{bmatrix} \varepsilon_x - \frac{\varepsilon_v}{3} & \varepsilon_y - \frac{\varepsilon_v}{3} & \varepsilon_z - \frac{\varepsilon_v}{3} & \sqrt{2}\varepsilon_{xy} & \sqrt{2}\varepsilon_{yz} & \sqrt{2}\varepsilon_{zx} \end{bmatrix}^T \tag{2.4}$$

The geotechnical sign convention where a compressive load is denoted as positive is used for this work.

The relation between the volume change $\Delta\varepsilon_v$ of a material and the change in mean effective stress $\Delta p'$ is often assumed to be isotropic and given by the effective bulk modulus K' as:

$$\Delta p' = K' \Delta \varepsilon_v \tag{2.5}$$

and the relation between the increments in deviatoric stress and strain by the shear modulus G:

$$\Delta \boldsymbol{\sigma'}_d = 2G \Delta \boldsymbol{\varepsilon}_d \tag{2.6}$$

At small strain magnitudes, the relation between K and G are interrelated by the effective Young's modulus E' and the corresponding effective Poisson's ratio ν':

$$K' = \frac{E'}{3(1-2\nu')} \qquad\qquad G = \frac{E'}{2(1+\nu')} \tag{2.7}$$

The stiffness of soft natural clays is non-linear, see Figure 2.1a, with a stiffness that depends on the current effective stress state and can be approximated by a linear strain logarithmic stress relation (Cummings et al. 1950; Burland 1990). Soft natural clays also show a distinct yield behaviour. The most established approach is to separate the small elastic (reversible) strain below yield and the large plastic non-reversible strains beyond yield. The plastic response is significantly softer compared to the elastic response. The yield stress (represented by the apparent preconsolidation pressure in 1D) in soft natural clays results from historic loading (changes in effective stress, creep and cementation). Additional factors influence the yield stress, which will be elaborated on in the following sections. Natural soils have been shown to be significantly stiffer for small strains compared to large strains as measured in conventional laboratory testing (Dobry and Vucetic 1987; Clayton 2011), see Figure 2.1b, which also denotes typical threshold values for the strain delimiting the elastic and plastic response of clays.

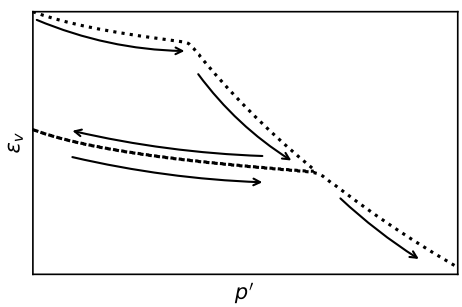

(a) *Idealised volumetric elastoplastic response with a stress dependent stiffness.*

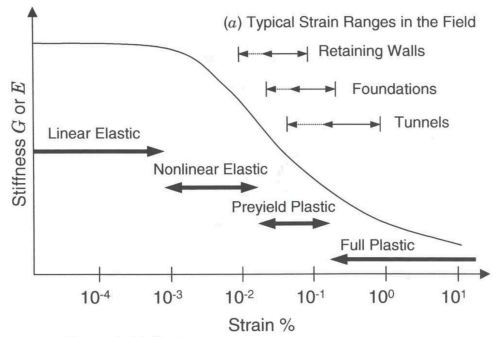

(b) *Idealised strain amplitude dependent stiffness. Mitchell and Soga (2005)*

Figure 2.1: *Stiffness of clay.*

The initial response of saturated clays upon load application is often in the undrained regime, where excess pore water pressures completely carry the applied load. Over time, consolidation occurs, during which excess pore water pressures dissipate, consequently increasing the effective stress in the soil. The stiffness of clay upon undrained loading can be understood by adopting

an undrained modulus E_u and letting the Poisson's ratio $\nu \rightarrow 0.5$ (by definition constant volume response) in the stiffness Equations 2.7, leading to, in theory, infinite bulk stiffness. The water in the pores does not resist shear, hence, in undrained conditions $G_u = G$.

2.2 Yielding

The yield stress of soft natural clay stems from the intrinsic properties of the soil, in combination with the historic effective stress levels and direction of loading. Commonly, natural clays are deposited in water vertically, forming horizontal layers, resulting in an anisotropic stress environment (Mitchell and Soga 2005). The overburden load and pore water conditions dictate the magnitude of the vertical (effective) stress, while the horizontal effective stress results from a combination of the current vertical effective stress, the mechanical behaviour of the clay and the stress history (Mayne and Kulhawy 1982).

The loading direction and initial stress conditions have been found to influence the deviatoric stress at failure for soft natural clays. Loading rate also matters, as will be discussed in Section 2.3. Systematic stress probing in multiple directions at a single loading rate has been conducted by, *e.g.*, Sällfors (1975), Larsson (1977), Graham et al. (1983), Leroueil and Vaughan (1990), Wheeler et al. (2003), and Koskinen (2014), on different natural clays. When combined, the yield points from different stress paths form an inclined yield surface characterised by a higher yield stress in compression than in extension. Furthermore, the size of the inclined yield surface has been shown to be strongly related to stress history which is commonly quantified using the yield stress (apparent preconsolidation pressure) in the oedometric loading path σ'_{vc}.

An example of the yield surface of an anisotropic natural soft clay is exemplified in Figure 2.2 with data from Graham et al. (1983). The results are presented in the simplified cross anisotropic triaxial stress space p' vs. q, defined as $p' = (\sigma'_v + 2\sigma'_h)/3$ and $q = (\sigma_v - \sigma_h)$, and include the yield points from triaxial stress probing on soil from four different depths. When the data are normalised with the σ'_{vc}, the yield points collapse in a narrow band that forms a normalised inclined yield surface. Although different soft natural clays share the characteristics of anisotropy and a stress-dependent yield surface, the shape of the surface is unique for each clay and can be identified by systematic effective stress probing in relevant isotropic and deviatoric stress paths.

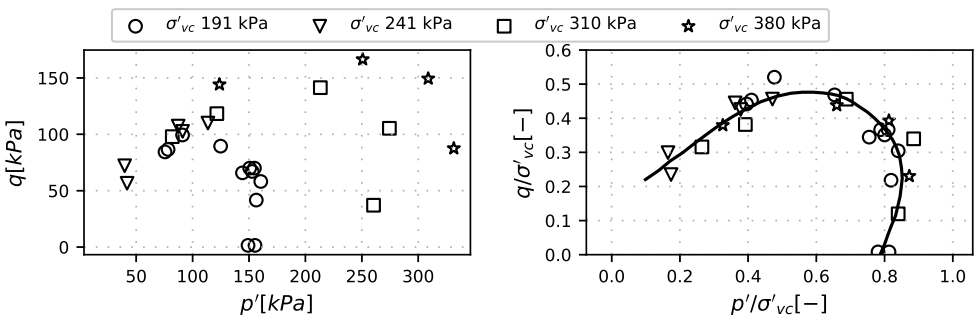

Figure 2.2: *Normalised yield surface of a soft natural clay from Winnipeg. Based on triaxial test data on clay sampled from four depths, data from Graham et al. (1983).*

2.3 Material rate-dependency

Soft natural clays exhibit a strain rate-dependent response, sometimes called viscous effects, which manifests as i) rate-dependent yield stress and undrained strength, ii) creep, *i.e.*, continuous deformation on sustained loading, and iii) stress relaxation at a constant deformation. The size of the yield surface of a natural clay relates to the apparent preconsolidation pressure that is evaluated in oedometric loading conditions (vertical effective stress - void ratio). The influence of rate-dependency is often discussed in the oedometric loading conditions but is equally applicable to the rate-dependent behaviour of clay in other loading paths, see *e.g.*, Tavenas et al. (1978).

Sällfors (1975) conducted Constant Rate of Strain tests (CRS) on a soft natural clay at different strain rates, see Figure 2.3, where an increase in strain rate was shown to lead to higher σ'_{vc}. When normalised with the evaluated σ'_{vc} of each test, the curves collapse. This indicates that the change in the yield stress due to a change in the strain rate is sufficient to map the stress-strain behaviour of the soil at different loading rates. Creep is defined as the time-dependent deformations that occur at constant effective stress. If put in the context of strain rate, the creep can be interpreted as a gradual reduction of strain rate over time. Leroueil et al. (1985) conducted a series of oedometer creep tests on Batiscan clay. The deformations were recorded at various times, converted to strain rates, and used to illustrate the stress-strain response for the clay corresponding to the various strain rates, see Figure 2.4a. The results provide very similar curves to the influence of strain rate observed for the CRS test results in Figure 2.3.

Relaxation, *i.e.*, the reduction in effective stress under constant deformations is governed by the same mechanism as creep but instead of constant load, the deformations are kept constant, resulting in a reduction of effective stress. In the context of strain rate, relaxation can be seen as a reduction in strain rate under constant volume. Larsson (1977) studied the undrained relaxation of soft natural clay using triaxial creep tests. The clay samples were consolidated to an initial stress state based on the *in-situ* stress state of the soil. Subsequently, the samples were rapidly loaded in axial compression to varying levels of mobilisation. After the rapid loading, the test were left in undrained conditions. The response during the undrained stress relaxation, see Figure 2.4b, results in a reduction of effective stress, and a corresponding increase in pore water pressures. During the relaxation process, the three tests with the largest deviator stress failed.

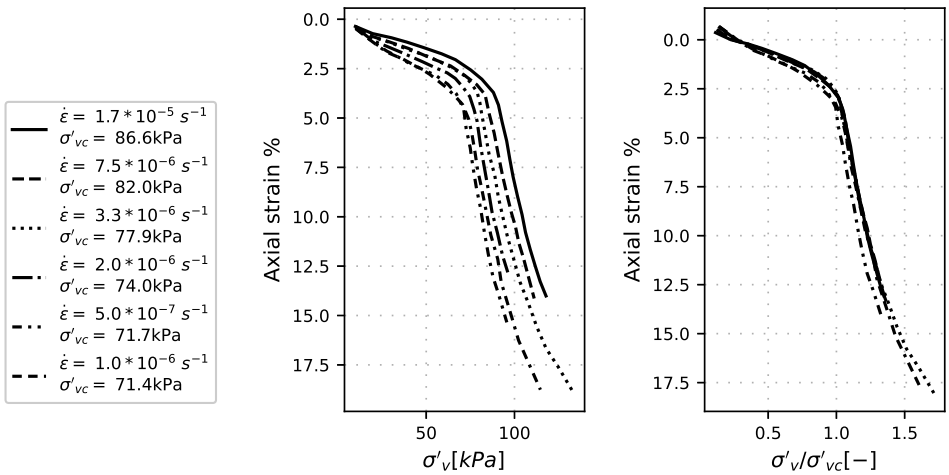

Figure 2.3: *Influence of loading rate on the stress strain response of a soft natural clay. CRS tests at different strain rates $\dot{\varepsilon}$ on result in different vertical yield stress σ'_{vc}. Tests was conducted on clay from Bäckebol by Sällfors (1975).*

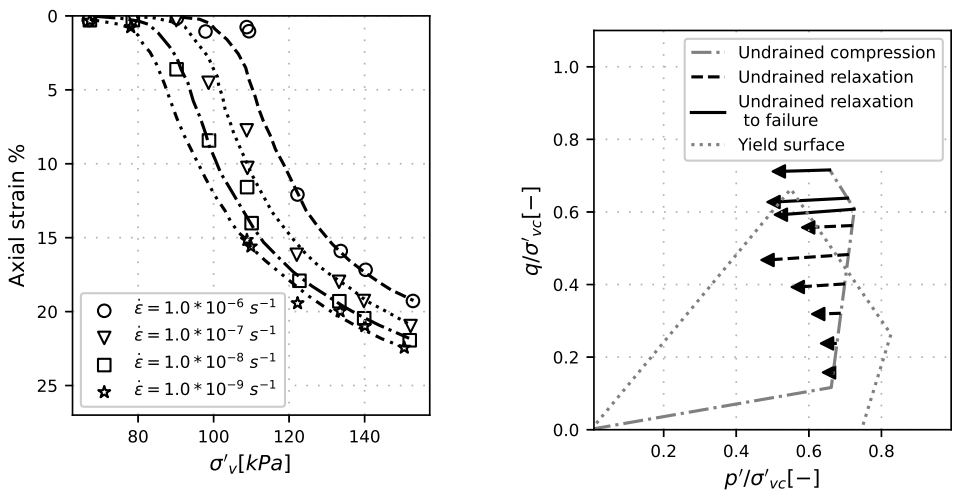

(a) *Oedometric creep tests. Stress-stain relation for various strain-rates (load step duration), data from Leroueil et al. (1985).*

(b) *Relaxation of effective stress in undrained conditions, data from Larsson (1977).*

Figure 2.4: *Rate dependent response of clay.*

2.4 Apparent bonding

In their natural state, soft clays resist higher loads than in their reconstituted state at the same void ratio (an imaginary state), which is attributed to some apparent bonding in the clay (Burland 1990). This phenomenon was studied by Leroueil (1996) on re-sedimented Jonquière Clay that was left for 128 d in an oedometer cell under a constant load, see Figure 2.5. After 128 d, the sample showed an increase in yield stress (apparent preconsolidation pressure) compared to the response of soil tested without the sustained load step, which is partly attributed to the creep of the soil to a denser state (lower void ratio e). However, the influence of creep is limited to the increase in the yield stress found up to the normal compression line (NCL). The additional difference in the yield stress is attributed to the development of some apparent bonding in the soil. The term ageing is commonly used to discuss the additional increase in pile capacity after the end of consolidation, which includes, but is not limited to, creep and the development of some apparent bonding (Doherty and Gavin 2013).

When loading continues past yielding, the inclination of the compression line is initially steeper for the intact natural clay, which results from the gradual destruction of the bonding in the soil. The curves of the bonded and (unbonded) remoulded soil will ultimately converge at large values for vertical effective stress when the clay has reached a completely destructured state (Leroueil et al. 1979; Koskinen et al. 2002).

The sensitivity, *i.e.*, the ratio of the intact peak undrained shear strength and the remoulded undrained shear strength (Mitchell and Soga 2005), is usually used to measure the potential for strain softening of a natural clay due to remoulding. In the Nordic countries, the fall cone test (where the penetration is linked to the shear strength) is most commonly used to determine the sensitivity, by first testing the clay sample in its intact state, before remoulding it and retesting. The sensitivity is closely linked to the amount of bonding in the soil, however, the bonding is quantified in a known state, *i.e.*, void ratio and stress, whereas the state of the clay during the fall cone test is unknown. When formulating the constitutive models in Section 2.6, the loss of (apparent) bonding as a result of plastic strains is called destructuration.

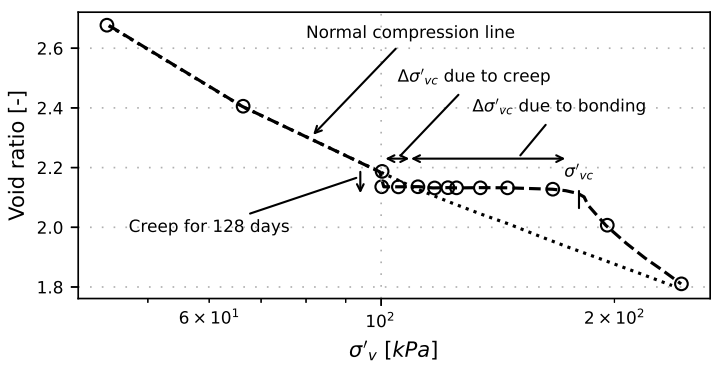

Figure 2.5: *Influence of creep and bonding on the oedometric response of resedimented Jonquière Clay, data from Leroueil (1996).*

2.5 Critical state in clays

The concepts of critical state soil mechanics are based on the systematic testing of reconstituted clays subjected to various levels of isotropic preloading (Roscoe et al. 1958). The framework stipulates that soils, when sheared past the point of yielding, ultimately reach a critical state CS at which further shearing of the soil will occur under a constant stress ratio and volume. The critical state line CSL is defined by its slope M_c in compression and M_e in extension which defines the relation between p' and q at critical state for a given soil, see Figure 2.6.

Depending on the relation between the yield surface of the soil, the initial stress state, and the stress path towards failure, the soil will reach yield at different sides of the CSL. When the soil reaches yield at a point on the right-hand side of CSL, at the "wet side", it contracts on its way to CS, which results in volumetric hardening in drained triaxial loading and the generation of positive excess pressures in undrained loading. In contrast, if the soil reaches yield at a point on the left-hand side of CSL, at the "dry side", the soil will dilate on its way to CS, resulting in dilation (increase in volume) in drained loading or the generation of negative excess pore water pressures (suction) in undrained loading.

Allman and Atkinson (1992) conducted triaxial tests on K_0 consolidated reconstituted soil with various degrees of unloading before loading in extension or compression in both undrained and drained conditions. The results from the tests are presented in Figure 2.6 and clearly illustrate the existence of a critical state that is reached independently of the initial state of the soil and the drainage conditions. The inclination of CSL in compression is higher than in extension.

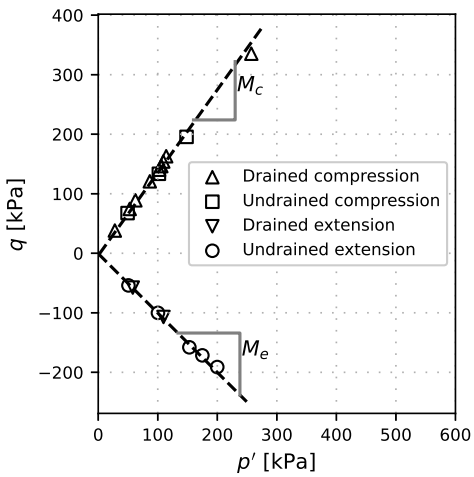

Figure 2.6: *Critical state line in compression and extension. Data from drained and undrained triaxial test on Bothkennar clay presented by Allman and Atkinson (1992).*

2.6 Generalised behaviour of soft natural clays

The concept of critical state soil mechanics (Roscoe et al. 1958) provides the basis of the generalised framework describing the stress-strain response of soft natural clays. Critical state soil mechanics, in combination with insights from the experiments on the yielding behaviour of clays, resulted in the formulation of the elastoplastic Modified Cam Clay (MCC) model (Roscoe and Burland 1968). Since then, critical state soil mechanics has been used to develop increasingly more advanced constitutive models for natural clays. In the following, the critical state models SCLAY1S and Creep-SCLAY1S will be used to generalise the behaviour of soft natural clays.

The formulation of the (Creep-)SCLAY1(S) models is based on MCC, *e.g.*, Roscoe and Burland (1968) and Wood (1990), and was gradually extended to include anisotropy and evolution of anisotropy (SCLAY1, Wheeler et al. (2003)), bonding and destructuration (SCLAY1S, Koskinen et al. (2002)). Creep-SCLAY1S is a viscoplastic formulation of SCLAY1S that incorporates the rate-dependent nature of soft soils (Sivasithamparam et al. 2015b; Gras et al. 2018). A small strain formulation has also been used in combination with Creep-SCLAY1S, see *e.g.*, Tahershamsi et al. (2023).

SCLAY1S and Creep-SCLAY1S are both formulated in a hierarchical manner, see Table 2.1. Hence, both the elastoplastic and viscoplastic model families allow for studying the influence of the additional features (anisotropy and bonding) beyond the basic framework (MCC). Furthermore, the influence of rate-dependency can be studied by comparing the response captured by SCLAY1S and Creep-SCLAY1S.

The models have been successfully used to capture various problems, *e.g.*, the response of excavations (Tornborg et al. 2021; Bozkurt et al. 2023; Tornborg et al. 2023), embankments (Amavasai et al. 2018), pile installation (Karlsson et al. 2019), installation of stone columns (Castro and Karstunen 2010) and slope stability (Sellin and Karstunen 2023).

Table 2.1: Hierarchical model features of SCLAY1S and Creep-SCLAY1S

Model	Basic framework	Anisotropy	Rotation	Bonding
SCLAY1S	Elastoplastic	Yes/No	Yes/No	Yes/No
Creep-SCLAY1S	Viscoplastic	Yes/No	Yes/No	Yes/No

Some definitions

Before describing the model some definitions related to the formulation need to be made. The Cauchy stress tensor (see equation 2.1), with the y-axis as the vertical direction is used in combination with the strain rate tensor defined as:

$$\dot{\boldsymbol{\varepsilon}} = \begin{bmatrix} \dot{\varepsilon}_x & \dot{\varepsilon}_y & \dot{\varepsilon}_z & \dot{\varepsilon}_{xy} & \dot{\varepsilon}_{yz} & \dot{\varepsilon}_{zx} \end{bmatrix}^T \tag{2.8}$$

The deviatoric stress tensor is defined as:

$$\boldsymbol{\sigma'}_d = \begin{bmatrix} \sigma'_x - p' & \sigma'_y - p' & \sigma'_z - p' & \sqrt{2}\tau_{xy} & \sqrt{2}\tau_{yz} & \sqrt{2}\tau_{zx} \end{bmatrix}^T \tag{2.9}$$

where the mean effective stress is $p' = (\sigma'_x + \sigma'_y + \sigma'_z)/3$. The deviatoric strain rate tensor is defined as:

$$\dot{\boldsymbol{\varepsilon}}_d = \left[\dot{\varepsilon}_x - \frac{\dot{\varepsilon}_v}{3} \;\; \dot{\varepsilon}_y - \frac{\dot{\varepsilon}_v}{3} \;\; \dot{\varepsilon}_z - \frac{\dot{\varepsilon}_v}{3} \;\; \sqrt{2}\dot{\varepsilon}_{xy} \;\; \sqrt{2}\dot{\varepsilon}_{yz} \;\; \sqrt{2}\dot{\varepsilon}_{zx}\right]^T \tag{2.10}$$

where $\dot{\varepsilon}_v = (\dot{\varepsilon}_x + \dot{\varepsilon}_y + \dot{\varepsilon}_z)$. A deviatoric fabric tensor is defined as:

$$\boldsymbol{\alpha} = \left[\alpha_x - 1 \;\; \alpha_y - 1 \;\; \alpha_z - 1 \;\; \sqrt{2}\alpha_{xy} \;\; \sqrt{2}\alpha_{yz} \;\; \sqrt{2}\alpha_{zx}\right]^T \tag{2.11}$$

where the components have the property:

$$\alpha_x + \alpha_y + \alpha_z = 3 \tag{2.12}$$

The formulation of the slope of the critical state line is stress path dependent. The Lode angle θ dependent formulation of $M(\theta)$ follows Sheng et al. (2000) as:

$$M(\theta) = M_c \left(\frac{2m^4}{1 + m^4 + (1 - m^4)\sin 3\theta_\alpha}\right)^{1/4} \tag{2.13}$$

where $m = M_c/M_e$ and:

$$\sin 3\theta_\alpha = -\left[\frac{3\sqrt{3}}{2}\frac{(\boldsymbol{J}_3)_\alpha}{(\boldsymbol{J}_2)_\alpha^{3/2}}\right] \tag{2.14}$$

The $(\boldsymbol{J}_2)_\alpha$ and $(\boldsymbol{J}_3)_\alpha$ are the second and third invariants of the modified deviatoric stress ($\boldsymbol{\sigma'}_d - \boldsymbol{\alpha}_d p'$), see *e.g.*, Sivasithamparam et al. (2015b).

2.6.1 Creep-SCLAY1S

A detailed description of the viscoplastic Creep-SCLAY1S model will be presented in the following Section. The formulation of SCLAY1S, which is an equivalent standard elastoplastic model will not be elaborated, and the reader is referred to Koskinen et al. (2002). Since the models rely on similar hardening laws, SCLAY1S can conceptually be understood by replacing viscoplastic strains with plastic strains and the Normal Compression Surface with a yield surface. However, in the elastoplastic version of the model, the current effective stress state cannot fall outside the yield surface.

The viscoplastic critical state model Creep-SCLAY1S is formulated around three surfaces that are identical in shape and orientation but different in size, see Figure 2.7. The model is formulated such that at any stress state, the total strain rate is a combination of elastic (e) and viscoplastic or creep (c) strain rates:

$$\dot{\varepsilon} = \dot{\varepsilon}^e + \dot{\varepsilon}^c \tag{2.15}$$

The Current Stress Surface (CSS) describes the current stress state of the soil and its size is controlled by the equivalent mean effective stress p'_{eq} at the hydrostatic axis. The Normal Compression Surface (NCS) forms the boundary between large and small creep rates, which would be called a yield surface in a rate-invariant model. The size of the NCS is expressed by the isotropic

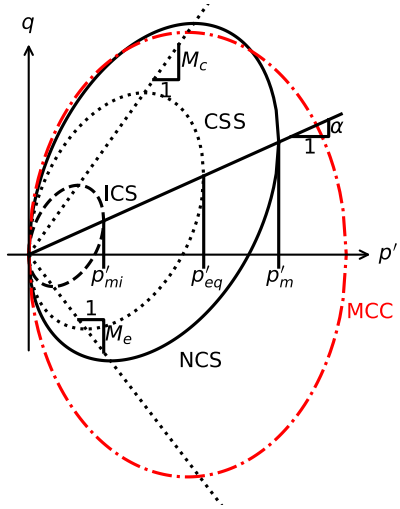

Figure 2.7: *Illustration of Creep-SCLAY1S model surfaces in simplified triaxial space.*

preconsolidation pressure p'_m. The Intrinsic Compression Surface (ICS) represents an imaginary yield surface of the soil at a state without bonding, inspired by Gens and Nova (1993) and with a size defined by the intrinsic isotropic pre-consolidation pressure p'_{mi}. The sizes of NCS and ICS are linked by the bonding parameter χ according to the relation $p'_m = (1+\chi)p'_{mi}$. The surfaces are defined by the expression:

$$f = \frac{3}{2}\left[\{\boldsymbol{\sigma'}_d - p'\boldsymbol{\alpha}_d\}^T\{\boldsymbol{\sigma'}_d - p'\boldsymbol{\alpha}_d\}\right] - \left[M(\theta)^2 - \frac{3}{2}\boldsymbol{\alpha}_d^T\boldsymbol{\alpha}_d\right](p_{surf} - p')p' = 0 \qquad (2.16)$$

were p'_{surf} is the parameter controlling the size of the specific surface, *i.e.*, p'_m, p'_{eq} and p'_{mi}. The surfaces of the model are illustrated in simplified triaxial space p'/q in Figure 2.7 where $\sigma'_x = \sigma'_z$ and $q = (\sigma'_y - \sigma'_x)$. For reference, the yield surface corresponding to MCC initialised from the same stress state and apparent overconsolidation ratio OCR is included.

The scalar representation of the anisotropy α is the inclination of the yield surface in $p' - q$ space with regards to the mean effective stress axis where $\alpha^2 = \frac{3}{2}\boldsymbol{\alpha}_d^T\boldsymbol{\alpha}_d$. The initialisation of the model is based on assuming cross anisotropy in the 3D space, so that the initial inclination of the surfaces is defined by the scalar value α_0 and the following relations:

$$\alpha_x = \alpha_z = 1 - \frac{1}{3}\alpha_0 \qquad \alpha_y = 1 + \frac{2}{3}\alpha_0 \qquad \alpha_{xy} = \alpha_{yz} = \alpha_{zx} = 0 \qquad (2.17)$$

The Creep-SCLAY1S model contains three hardening laws: one corresponding to volumetric hardening similar to MCC, one corresponding to the rotation of NCS similar to SCLAY1, and one corresponding to the destructuration of the bonding similar to SCLAY1S.

The rotational hardening law is defined as:

$$\dot{\boldsymbol{\alpha}}_d = \omega \left(\left[\frac{3\boldsymbol{\sigma'}_d}{4p'} - \boldsymbol{\alpha}_d \right] \langle \dot{\varepsilon}_v^c \rangle + \omega_d \left[\frac{\boldsymbol{\sigma'}_d}{3p'} - \boldsymbol{\alpha}_d \right] |\dot{\varepsilon}_d^c| \right) \tag{2.18}$$

where $\langle \dot{\varepsilon}_v^c \rangle = \dot{\varepsilon}_v^c$ if $\dot{\varepsilon}_v^c > 0$ and $\langle \dot{\varepsilon}_v^c \rangle = 0$ if $\dot{\varepsilon}_v^c < 0$ and $\dot{\varepsilon}_v^c$ is the deviatoric viscoplastic strain rate. The rate of rotation due to viscoplastic strain ω and the relative rate of rotation due to deviatoric viscoplastic strains ω_d control the rate of rotation. The value of ω needs to be calibrated based on experimental testing whilst ω_d can be theoretically derived from K_0^{NC} using the M_c.

The destructuration law changes the amount of bonding χ according to:

$$\dot{\chi} = -a\chi \left[|\dot{\varepsilon}_v^c| + b\dot{\varepsilon}_q^c \right] \tag{2.19}$$

where a is the volumetric rate of destructuration and b the rate of destructuration due to deviator strain. The volumetric hardening law changes the size of ICS:

$$\dot{p}'_{mi} = \frac{p'_{mi}}{\lambda_i^* - \kappa^*} \dot{\varepsilon}_v^c \tag{2.20}$$

where κ^* and λ_i^* are visualised in Figure 2.8 and are called modified swelling index and modified intrinsic compression index, respectively.

The (isotropic) elastic response of the model is similar to MCC where the effective elastic bulk modulus K' is based on κ^* ($K' = p'/\kappa^*$) and the effective elastic shear modulus G is calculated based on a constant value of Poission's ratio ν' according to $G = 3K'(1-2\nu')/2(1+\nu')$. The viscoplastic (creep) strains of the model are assumed to follow an associated flow rule, formulated as:

$$\dot{\varepsilon}_{ij}^c = \dot{\Lambda} \frac{\partial p'_{eq}}{\partial \sigma'_{ij}} \tag{2.21}$$

$$\dot{\Lambda} = \underbrace{\frac{\mu_i^*}{\tau_{ref}} \left(\frac{p'_{eq}}{p'_m} \right)^{\frac{\lambda_i^* - \kappa^*}{\mu_i^*}}}_{\text{i}} \underbrace{\left(\frac{M^2(\theta) - \alpha^2_{K_0^{nc}}}{M^2(\theta) - \eta^2_{K_0^{nc}}} \right)}_{\text{ii}} \tag{2.22}$$

where i) controls the creep strain rate and ii) is added to ensure that the resulting creep strain rate in oedometric conditions corresponds to the measured volumetric creep strain rate. The reference time of the viscoplastic formulation τ_{ref} corresponds to the duration of the test used to define the size of the NCS surface, most commonly an oedometer test with the load step duration of 24 h, *i.e.*, one day.

2.6.2 Small strain formulation

A small strain formulation following Sivasithamparam et al. (2021) has been recently incorporated with the Creep-SCLAY1S model. Details on the implementation are presented in Tahershamsi

et al. (2023). The Creep-SCLAY1S model, in combination with this small strain formulation, will be denoted as Creep-SCLAY1Sss in this work.

The formulation is based on Hsieh et al. (2017) and relates the current shear modulus G to the shear modulus at small strains G_0 according to:

$$G(\varepsilon_q) = G_0 \left[1 - \frac{\langle \varepsilon_q - \varepsilon_s \rangle}{A + B\langle \varepsilon_q - \varepsilon_s \rangle} \right] \tag{2.23}$$

where ε_q is the deviatoric strain invariant, ε_s is a threshold strain below which $G = G_0$, in this work $\varepsilon_s = 10^{-5}$ is assumed.

Parameters A and B are model parameters where A specifies the shape of the stiffness degradation curve, see Figure 2.1b, and B defines the relation between the small strain and large strain stiffness. By rearranging Equation 2.23 and letting ε_q approach to infinity:

$$\frac{G}{G_0} = 1 - \frac{1}{B} \tag{2.24}$$

Following Tahershamsi et al. (2023), for simplicity, B is replaced by a small strain multiplier ϖ as the input model parameter, controlling the relation between the small strain stiffness and the unloading reloading modulus at engineering strain levels G_{ur} as:

$$\varpi = \frac{G_0}{G_{ur}} \tag{2.25}$$

2.6.3 Some comments on Creep-SCLAY1S

The use of the Creep SCLAY1S model requires in total 14 model parameters (+2 for small strain stiffness formulation), see Table 2.2. The parameters can be divided into intrinsic model parameters that control the intrinsic (state-independent) behaviour of the material, state parameters describing the initial and current state, and the hardening parameters describing the evolution of the bond degradation and anisotropy in the soil.

The viscous behaviour in Creep-SCLAY1S is formulated using the intrinsic creep index of the soil. The creep rate can, in the context of strain rate, be seen as the vertical distance between two curves representing different strain rates, following the concepts of isotaches (Šuklje 1957), as seen in, *e.g.*, Figure 2.3. As such, this viscous formulation is able to capture the influence of the loading rate on the yielding of the soil as represented by the difference in σ'_{vc} due to the variation in strain rate. The aspects related to the rate-dependency of the model are illustrated in Figure 2.8 considering both strain-rate effects and creep.

Note that when changing from Creep-SCLAY1S to SCLAY1S λ_i^* and κ^* should be replaced by λ_i and κ using the relations

$$\lambda_i^* = \frac{\lambda_i}{1+e} \qquad\qquad \kappa^* = \frac{\kappa}{1+e} \tag{2.26}$$

Additionally, in simulations where bonding is not included in the analysis, λ_i^* should be replaced by a compression index representative for the relevant loading situations, commonly the λ^* evaluated at stress levels just beyond the apparent preconsolidation pressure (Figure 2.8).

Table 2.2: Creep-SCLAY1S model parameters. Parameters for the small strain stiffness formulation in parenthesis.

Basic behaviour	
λ_i^*	Modified intrinsic compression index [-]
κ^*	Modified swelling index [-]
ν'	Poisson's ratio [-]
M_c	Slope of CSL in compression [-]
M_e	Slope of CSL in extension [-]
μ^*	Modified intrinsic creep index [-]
(ϖ)	Small strain multiplier [-]
Initial state	
e_0	Initial void ratio [-]
α_0	Initial anisotropy [-]
χ_0	Initial amount of bonding [-]
OCR	Apparent overconsolidation ratio [-]
τ	Reference time for preconsolidation pressure [days]
Hardening behaviour	
ω	Rate of rotation [-]
ω_d	Relative rate of destructuration due to deviatoric strains [-]
a	Rate of destructuration [-]
b	Relative rate of destructuration due to deviatoric strains [-]
(A)	Shape factor for small strain stiffness degradation [-]

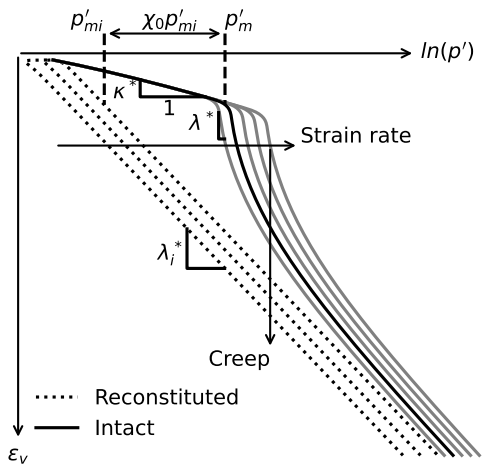

Figure 2.8: *Rate-dependent volumetric response of the Creep-SCLAY1S model.*

2.7 Coupled response of soil

The soft natural clays considered are assumed to be fully saturated within the context of this thesis. Thus, the response of the soil emerges from the interplay between the mechanical properties of the clay, discussed in the previous Sections, and the drainage properties. Two limit states, the drained and undrained state, are commonly adopted in geotechnical engineering. The drained situation relies on immediate dissipation of pore water pressures, while the undrained state assumes no dissipation of pore water pressures. Consequently, in the undrained conditions a practically constant volume response emerges, due to the high stiffness of the pore water. This undrained limit state can be numerically captured by letting Poisson's ratio $\nu \rightarrow 0.5$, which results in very high K, see equation 2.7.

The two-phase nature of saturated clays leads to a coupled response governed by a combination of the mechanical and hydraulic properties of the soil. Water is unable to transfer any shear stress while being almost incompressible when subjected to pure isotropic loading. In the short-term undrained limit state, any isotropic stress increase resulting from the external load is thus completely carried by pore water, resulting in the emerging excess pore water pressures as a result of negligible flow of pore water. In contrast, the shear stresses induced by the external load are instantaneously applied to the soil skeleton. Over time, the excess pore water pressures generated due to the loading dissipate, which correspondingly increases the effective stress and in turn changes the volume in the soil. After full dissipation of the pore water pressures, in the drained limit state, the external load is completely carried by the soil skeleton as an effective stress. The drainage response emerges from a combination of the emerging stiffness, the hydraulic conductivity of the soil, and the rate of external loading. It should be noted that the consolidation processes near a pile in clay during the installation and the subsequent equalisation is complex, opposed to oedometric conditions, as the excess pore water pressures generated during pile installation will dissipate under non-constant total stress.

During pile installation, the drainage situation in the soil emerges depending on the installation velocity (rate) v and the diameter of the pile d, in combination with the hydromechanical properties of the soil as captured by the combination of the vertical and horizontal consolidation coefficients c_v and c_h respectively. The consolidation coefficients in the soil result from the evolving compression moduli and hydraulic conductivity k of the soil.

The drainage situation in the soil during pile installation can be estimated by the non-dimensional normalised penetration velocity defined as $V = \frac{vd}{c_v}$. The consolidation coefficient can be estimated using the relation $c_v = \frac{k_v(1+e_0)\sigma'_{v0}}{\lambda\gamma_w}$ following Schneider et al. (2007) where γ_w is the unit weight of water.

In simple terms, this implies that the faster a pile is pushed into the soil, compared to the ability of the soil to accommodate the volume change (as represented by the rate of consolidation), the more likely it is that the emerging soil response will be undrained. The normalised response of the emerging penetration resistance (q_{net}) and excess pore pressures (Δu_2) are illustrated in Figure 2.9a for the penetration of a piezocone (CPTu) into normally consolidated kaolin during a geotechnical centrifuge test (Schneider et al. 2007). At low V the response is practically drained, no excess pore water pressure is developed. At intermediate V, an increase in penetration velocity

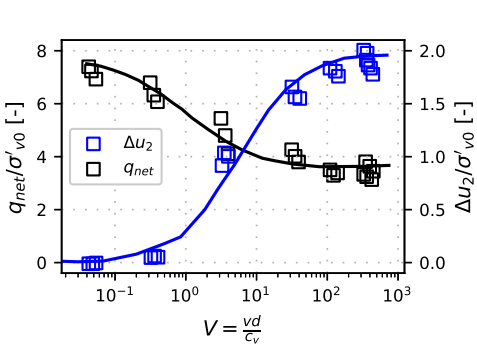

(a) *Influence of normalised penetration velocity on the drainage response of soil. Data from CPTu in kaolin clay (Schneider et al. 2007).*

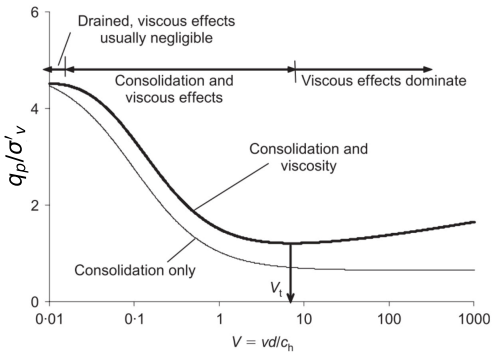

(b) *Combined influence of material rate-dependency and drainage. Illustrated by the penetration resistance as a function of normalised penetration velocity, Figure from Lehane et al. (2009).*

Figure 2.9: *Rate-dependent penetration response in clay.*

result in an increase in the excess pore pressure developed. At high V, the response is essentially undrained, and an additional increase in penetration velocity does not cause any additional excess pore water pressure due to a higher penetration (loading) rate. The suggested limits for the drained and undrained response are $V \approx 0.3$ and $V \approx 30$ respectively (DeJong and Randolph 2012). The cone resistance increases when the drainage conditions change from undrained to drained, due to the effective stress increase in the soil, which enables the mobilisation of a larger shear strength.

In addition to the rate-dependency of the hydromechanical coupling (consolidation), the rate-dependency of the material itself (viscous behaviour) also influences the emerging penetration resistance. The combined rate effects were studied by Lehane et al. (2009) with CPTu, T-bar and Ball cone penetrometers. Figure 2.9b shows the influence of the relative influence of consolidation and viscous behaviour at different V. The influence of consolidation controls the response at intermediate V, manifesting in a lower penetration resistance q_p. When V increases, the viscous behaviour dominates the response, resulting in an increase in net penetration resistance at increasing V in the undrained regime. Noteworthy is that a V denoted V_T exists where the penetration resistance is the lowest, which emerges from the combined effects of undrained behaviour and a minimum increase in the resistance due to the viscous behaviour.

The dissipation response following undrained cone penetration was numerically studied at different locations at the shaft by Teh and Houlsby (1991). The development of excess pore water pressure Δu during dissipation is normalised with the excess pore water pressure directly after installation Δu_i and presented in Figure 2.10. Δu was shown to be uniquely dependent on the location at the shaft and the time factor $T = \frac{c_h t}{R^2}$, with $2R$ is equal to the diameter d. The dissipation close to the tip is faster, resulting from partial consolidation in the vertical direction, while points C, D, E, and F show a very similar dissipation due to the largely horizontal dissipation. The distribution of excess pore pressure normalised with the shear strength $\Delta u/c_u$ in the soil at $T = 0$ (undrained) and after some dissipation at $T = 5$ is visualised in Figure 2.11.

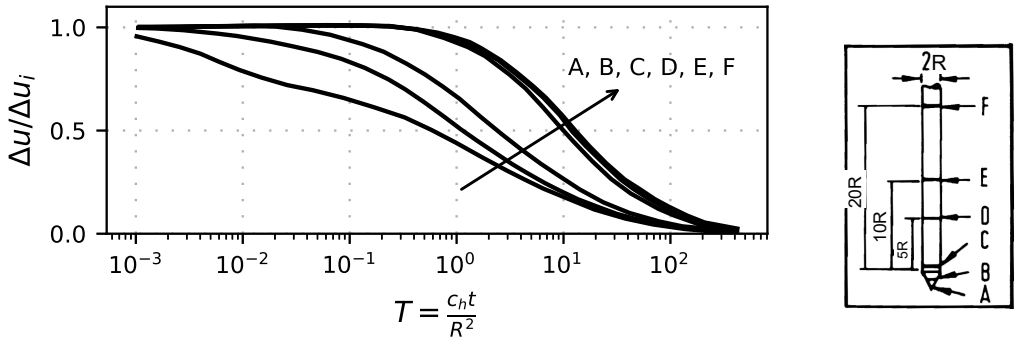

Figure 2.10: *Dissipation at the pile shaft after undrained CPTu penetration at different vertical distances from the tip, from Teh and Houlsby (1991).*

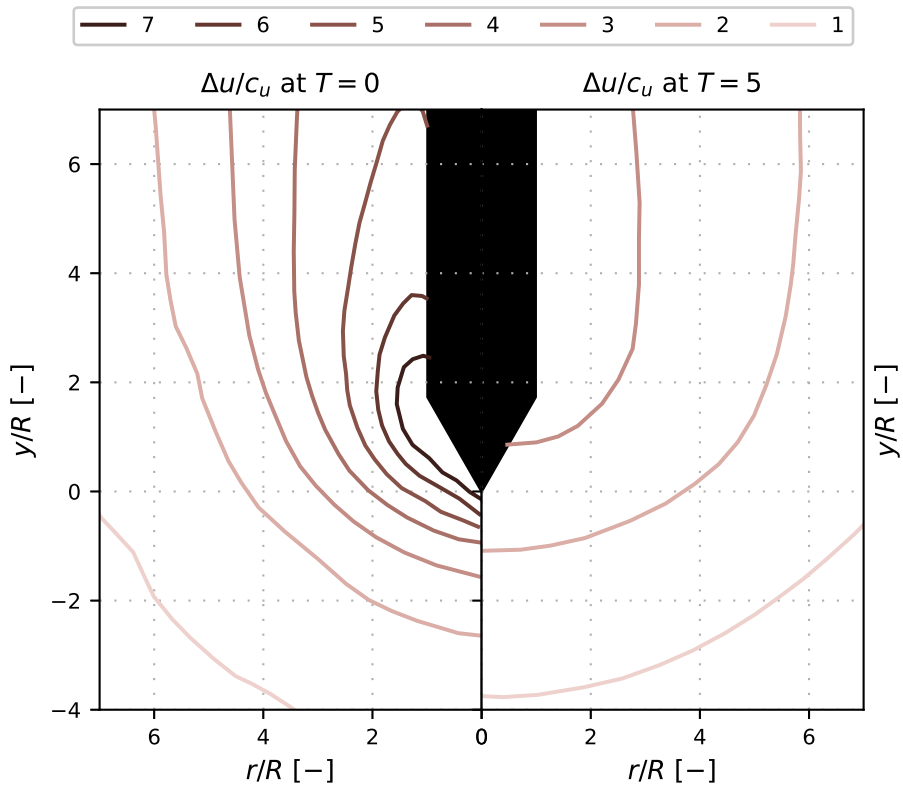

Figure 2.11: *Excess pore pressure following undrained cone penetration at $T = 0$ (undrained) and after some dissipation at $T = 5$, data from Teh and Houlsby (1991).*

3 Pile installation in soft clay

This Chapter elaborates on the impact of the installation of displacement piles in soft natural clays, considering the pile cycle introduced in Section 1.2. First, the influence of pile installation on the state of the pile-soil system is discussed, followed by an examination of the soil displacements resulting from pile installation.

3.1 Change of soil state

3.1.1 Shaft response

The emerging state of the soil at the shaft of a displacement pile governs the pile capacity in the pile cycle (Randolph 2003). During the largely undrained pile installation, the soft natural clay adjacent to the pile undergoes severe disturbance, *i.e.*, state change, due to shear-induced deformations. After pile installation, the state of the soil continues to evolve during the equalisation of the excess pore water pressures. Data on the evolution of the effective stress state at the pile shaft due to installation and subsequent equalisation of piles installed in natural clays was compiled by Karlsrud (2012). The data includes 14 test sites and more than 100 individual pile load tests. The measurements from soils with an $OCR < 2.5$ are included in Figure 3.1, where the data is plotted as a function of both OCR and plasticity index I_p. The results are presented as the stress ratio between the vertical *in-situ* effective stress σ'_{v0} and the horizontal effective stress σ'_h (denoted σ'_r when measured directly at the pile shaft) at different stages of the pile cycle. The stress ratios included are the *in-situ* earth pressure at rest K_0, the effective stress ratio directly after installation K_i and the effective stress ratio after consolidation K_c. Additionally, the change in total stress due to the installation of the pile is included by the term $K_i + \Delta u_i/\sigma'_{v0}$ where Δu_i is the excess pore water pressure measured directly after installation at the pile shaft.

Directly after installation, the stress state at the pile shaft is characterised by high excess pore water pressures, and reduced radial effective stresses compared to *in-situ*. During the equalisation, the excess pore water pressures dissipate, resulting in an increase in the effective stresses. Noteworthy is that during equalisation, a relaxation of total stress is present, which is different from the 1D oedometric consolidation case where the total stresses in the soil are constant throughout the consolidation process. The resulting K_c after consolidation is commonly found to be of similar magnitude to the estimated K_0.

In practical pile design, the failure load of piles is directly related to the *in-situ* strength of the clay see *e.g.*, Doherty and Gavin (2011), or to the CPTu test, see *e.g.*, Lehane et al. (2022). These methods are based on empirical relations which indirectly consider the installation effects, given that these piles are installed into the soil in which they are tested. The α_s method relates the shaft resistance at failure τ_f to the undrained shear strength of the soil $\alpha_s = \tau_f/s_u$ and the β method relates to the initial vertical effective stress as $\beta = \tau_f/\sigma'_{v0}$. Thus, the coefficients effectively incorporate the complex transient state of the pile-soil system over the installation and equalisation stages by the α_s or β without explicitly quantifying each stage. Figure 3.2 presents the α_s and β evaluated from the pile load test reported in Karlsrud (2012).

The influence of rate dependency on the emerging pile capacity was investigated by Brown et al. (2006), where the viscous response of the soil was shown to strongly influence the ultimate capacity

of the pile. The ageing of piles, *i.e.*, the increase in shaft capacity after the end of equalisation, was studied in Doherty and Gavin (2013) by retesting a pile after ten years. The conducted pile tests, in combination with a database study, suggests a continuous increase of pile capacity after the end of equalisation that can be captured by a linear capacity logarithmic time relation. Similar gain in pile capacity beyond equalisation was reported in Karlsrud et al. (2014) for loaded piles and was successfully modelled by using a combination of SSPM and an advanced constitutive model (Karlsson et al. 2019). The modelling suggests that the pile ageing is governed by relaxation and creep in the soil surrounding the pile.

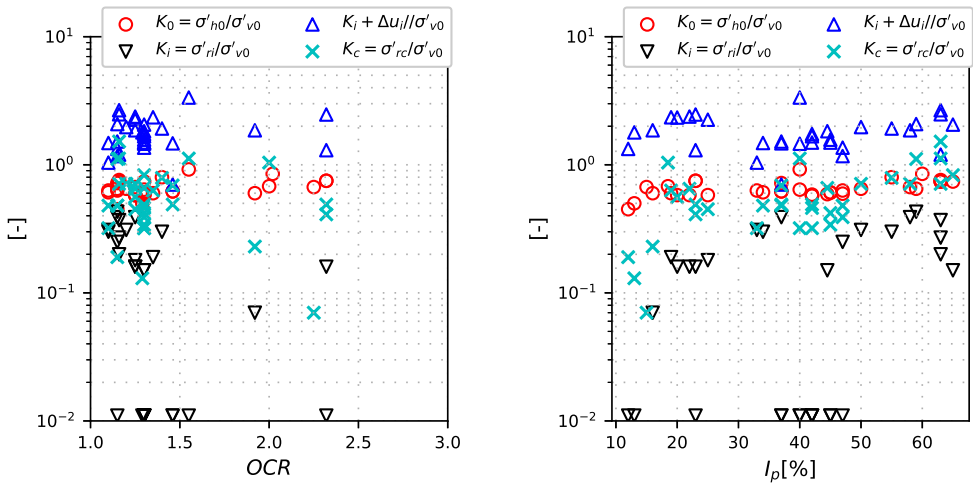

(a) (b)

Figure 3.1: *Evolution of radial stress at the pile shaft over the pile cycle as a function of OCR (a) and I_p (b), note that when $K_i < 10^{-2}$ the value is set to 10^{-2} to fit in the logarithmic axis. Data from Karlsrud (2012).*

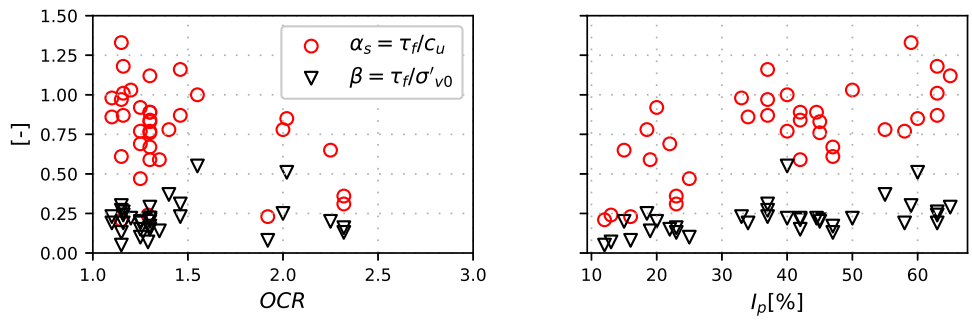

Figure 3.2: *Shaft capacity τ_f of piles, normalised with the undrained shear strength c_u (α_s), and with the in-situ vertical effective stress σ'_{v0} (β) as a function of OCR and I_p. Data from Karlsrud (2012).*

3.1.2 Soil response

The change in state from pile installation reaches beyond the soil directly adjacent to the pile shaft. Roy et al. (1981) measured the pore water pressures in the soil and at the pile shaft, both at the end of installation and during the equalisation stage. The measurements show, see Figure 3.3a, that the excess pore water pressures are highest at the pile shaft and decrease with the distance from the pile. The distance is measured from the pile shaft and normalised by the radius of the pile R. The magnitude of excess pore water pressures and the gradients in the distribution decrease with time, as included by the time factor $T = \frac{c_h t}{R^2}$ based on measurements at 0.25, 3, 22 and 70 h after pile installation. Interestingly, the pore water pressures at a distance exceeding $5R$ initially increase following the radial dissipation of pore pressures, at a distance of $19R$ from the pile, the pore pressures are higher at time $T = 10.51$ compared to $T = 0.04$. Similar observations are made in physical model tests at elevated stress levels in the geotechnical centrifuge by Ottolini et al. (2014).

The dissipation of pore water pressures following pile installation in soft natural clays results in a change in the effective stresses, and a corresponding volume change. The extent of this volume change was explored by Karlsrud and Haugen (1985) on a soil block extracted near a displacement pile, after equalisation, see Figure 3.3b. The void ratio after equalisation e was shown to be reduced compared to the void ratio of the in-situ soil e_0. Additionally, the figure includes the shear strain in the plane of the block face that was evaluated from the distortion of initially horizontal layers in the block. The disturbance resulted in a change in shear strength c_u to the soil (fall cone). The shear strength within $0.5R$ from the pile was increased in relation to the in-situ value c_{u0}. In contrast, a reduction of shear strength was found for soil at larger distances.

The change in state due to pile installation results in an immediate reduction of shear strength. Roy et al. (1981) report a reduction of vane shear strength to about 60 % to 75 % of the initial value, which is similar to the values reported by Bozozuk et al. (1978). No significant reduction was observed at distances greater than $6R$ from the pile. After the full equalisation, the measured vane shear strength was similar to the in situ shear strength at all distances from the pile. The shear strength of the disturbed soil after equalisation has been reported to be both slightly higher (Seed and Reese 1957) and lower (Cummings et al. 1950; Torstensson 1973; Bozozuk et al. 1978) than the initial shear strength. Furthermore, the stress-strain response measured on the samples extracted near an installed displacement pile shows clear evidence of a change in the compression behaviour. The yield stress is commonly slightly lower, combined with a less pronounced yield point and less evidence of destructuration (Torstensson 1973; Fellenius and Samson 1976; Hunt et al. 2002).

Hunt et al. (2002) provides a detailed investigation of the influence of pile installation on the state of the soil by comparing the response of samples extracted before pile installation and after installation and equalisation. The results of the CRS tests and the undrained triaxial compression tests are shown in Figure 3.4 and show clear evidence of strong disturbance due to the pile installation. Similar to the vane shear strength, the peak shear stress is comparable to the pre- and post-pile response. However, the strains required to reach the peak shear stress are considerably higher in the post-pile samples. Additionally, the post-peak softening behaviour of the pre-pile sample caused by the gradual destructuration of the clay is not visible in the post-pile sample, which implies that the post-pile sample lost all initial structure (bonding) due to the pile installation. The pre-pile soil response shows a distinct peak in deviator stress at a strain level of about 1 % to 2 %,

followed by a strain softening in combination with an increase in excess pore water pressures. In contrast, the post pile response shows a more ductile response with peak shear stress found at 5 % to 8 % without strain softening. The destructuration caused by the pile installation is also clear when examining the CRS response. An unstructured soil is expected to have a constant slope in the $\log(\sigma'_v)$–e space after the yield, while a structured soil has an initially softer response as illustrated in Figure 2.5. This distinct difference in the compression behaviour of structured and destructured soil is evident when comparing the CRS response of the pre-pile and post-pile samples. The response of the post-pile response after yielding shows a constant inclination of the compression line, while the pre-pile samples show an initially softer response and only stabilise at stresses beyond $5\sigma'_{v0}$, which indicates a destructured state in the post-pile sample.

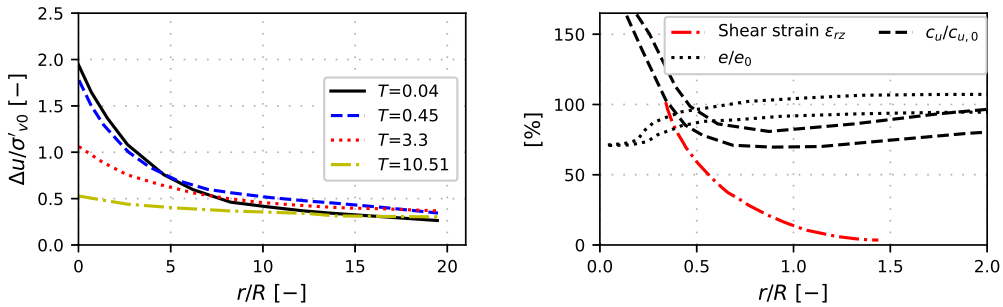

(a) *Evolution of pore pressure in the soil following pile installation in a soft natural clay. Data from Roy et al. (1981).*

(b) *Void ratio and shear strength after consolidation. Shear strain from a distorted layer of in a block sample. Data from Karlsrud and Haugen (1985).*

Figure 3.3: *Influence of pile installation on adjacent soil.*

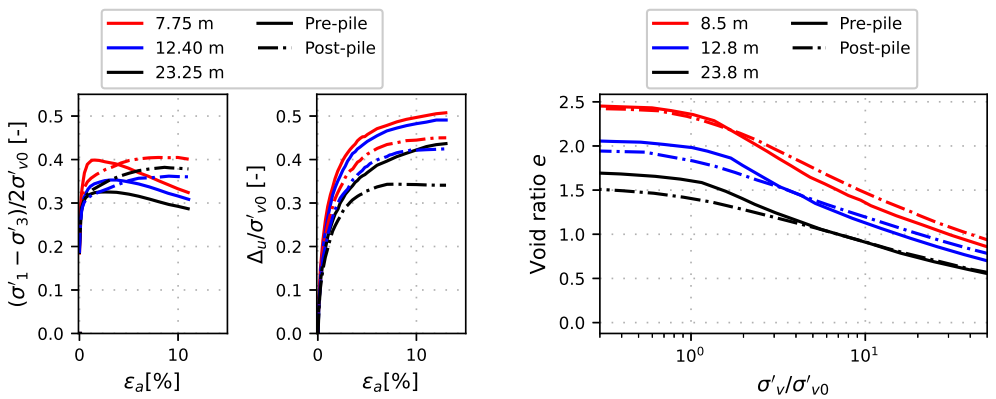

(a) K_0 *consolidated undrained triaxial compression test.*

(b) *Constant rate of strain test.*

Figure 3.4: *Stress-strain response of soft natural clay extracted pre-pile installation and post-pile installation. Data from Hunt et al. (2002).*

3.2 Mass-displacements due to pile installation in clay

The installation of a displacement pile into natural soft clay results in mass-displacements of soil away from the pile, see *e.g.*, Orrje and Broms (1967), Hagerty and Peck (1971), Bozozuk et al. (1978), and Edstam and Kullingsjö (2010). This displacement can be separated into the rigid body translation and rotation, and deformations (changes of shape by shear distortion or volume change). When the pile is installed into clay, the pile-soil system responds in an undrained manner, which prevents short-term volumetric deformations. However, large shear deformations of the soil are present.

The short-term soil displacements during the installation stage of the pile cycle have been studied in a laboratory environment by, *e.g.*, Gue (1984), Lehane and Gill (2004), Ni et al. (2010), Ottolini et al. (2014), and Zhou et al. (2017). These studies came to the same general conclusions: i) the displaced soil is equal to the installed pile volume, ii) soil movement decreases with the distance from the installed pile, iii) the soil displacements are strongly influenced by the presence of a stress-free surface.

A generalised axisymmetric method for the prediction of movements due to pile installation in clay was formulated by Sagaseta et al. (1997). The method called Shallow Strain Path Method (SSPM) is based on the assumption of an incompressible soil contained in a half-space with a stress-free ground surface. Sagaseta (2001) shows that SSPM produces a non-dimensional relation, see Figure 3.5, for small strain conditions for the displacements δ resulting from axisymmetric pile installation according to:

$$\frac{\delta L}{R^2} = \frac{\delta \pi L}{\Omega} = f(\frac{r}{L}, \frac{y}{L}) \tag{3.1}$$

where R is the radius of the pile, Ω is the cross-sectional area of the pile, L is the length of the pile.

The non-dimensional relation shows that the magnitude of displacements is scaled with Ω and L, and the distribution of the displacements relates to the relative vertical y/L and horizontal r/L position respectively. Zhou et al. (2017) investigated the influence of pile cross-sectional shape on the resulting displacements by comparing the results from an x-shaped with a cylindrical pile. The result indicates that the influence of shape is significant close to the pile and negligible at a distance greater than $5R_{eq}$ where the normalised displacements are independent of the cross-sectional shape.

Sagaseta (2001) compared the predictions of SSPM with published laboratory data and found an overall good agreement with the displacements due to the installation of a single pile. Since then, SSPM has been shown to be able to capture the magnitude of displacements from the installation of a single pile in physical model tests (Lehane and Gill 2004; Ni et al. 2010; Zhou et al. 2017) and for a single pile (Xu et al. 2006) and a pile group installation in the field (Edstam and Kullingsjö 2010). Given the basic assumptions of SSPM, the displacement fields from multiple piles can be added to predict the response from pile group installation which has been compared to field results from the installation of pile groups (Rehkopf 2001; Edstam and Kullingsjö 2010).

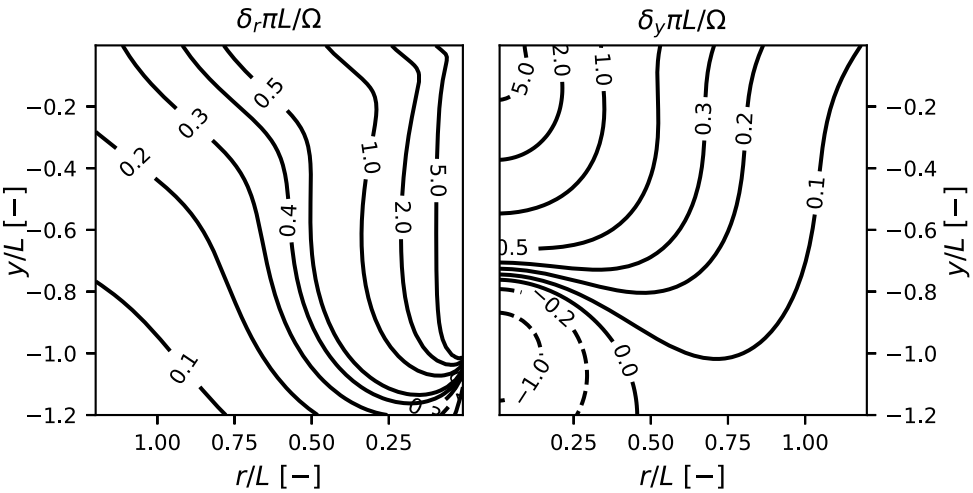

Figure 3.5: *Non-dimensional radial (r) and vertical (y) displacements δ due to axisymmetric pile installation in clay, obtained using Shallow Strain Path Method and the dimensionless response proposed by Sagaseta (2001).*

Influence from non-ideal soil and boundary conditions

Deviations from the generalised behaviour as expressed by SSPM are expected when the actual conditions differ from the basic assumptions of the method. The expected influence of deviations from the greenfield assumptions, *i.e.*, a horizontal ground surface, and an incompressible soil with a constant stiffness are:

- A limited domain size alters the distribution of soil displacements. A vertical boundary, *e.g.*, a side of a model container or a rock surface in the field, prevents horizontal displacement and increases vertical displacement in regions close to the boundary (Gue 1984). A horizontal boundary, *e.g.*, bedrock, increases the displacement close to the installed pile in the soil deposit. The effect increases with the decreasing distance between the pile and the horizontal boundary (Sagaseta 2001).

- Piles installed into sensitive clay are reported to result in lower displacements outside the area enclosed by a pile group in relation to the displacements when installed into a non-structured clay (Hagerty and Peck 1971; Massarsch 1976).

- The non-horizontal profile at the ground surface, *e.g.*, sloping ground and excavations, influences the distribution of soil displacements. Soil displacements are reported to increase in the downward direction of the slope. A concentration of movement is reported to happen at regions with lower elevation within a pile group (Hagerty and Peck 1971). Piling from within an excavation results in lower displacements outside the piling area (Dugan and Freed

1984).

- The presence of coarser soil, either as a layer or when piles are driven through the clay into underlying coarse-grained (frictional) soil, is resulting in deviations from the constant volume conditions observed for pile installation into clay (Turkel et al. 2023). Consequently, the observed vertical displacements are reduced due to compaction of coarse-grained soil, see *e.g.*, Hagerty and Peck (1971) and Bergdahl and Nilsson (1974).

- The dissipation of the pore water pressures at the equalisation stage of the pile cycle results in compression of the soil near the installed pile. The expected displacements due to consolidation at this stage is in the reversed direction from the displacements during installation, *i.e.*, radially towards the pile (Massarsch 1976; Pestana et al. 2002) and vertically downwards (Hagerty and Peck 1971; Massarsch 1976; Dugan and Freed 1984). Depending on the drainage conditions and the time frame of a construction project, partial consolidation can occur during the construction stage thus reducing the observed displacements.

Additional alterations of the greenfield conditions come from the presence of existing foundations. The stiffness of the structures causes a redistribution of the soil displacements compared to the greenfield conditions, affecting the distribution of displacements within the soil deposit. Some effects of existing foundations are:

- An existing single pile, when subjected to vertical soil movement, redistributes the soil displacements along its length, which results in relative displacements between the pile and the soil (Cooke and Price 1973). The vertical movement of the pile head is a result of the interaction between the distribution of soil displacements exerted on the length of the pile and the transfer of load at the pile shaft (Chow and Teh 1990). Typically, vertical displacements due to pile installation increase towards the surface, resulting in lower pile head displacements compared to the greenfield displacements of soil in the same location.

- The vertical displacements of existing structures on end bearing piles are reported to be significantly lower, $\approx 50\,\%$ than the measured ground displacements in a greenfield location at a similar distance from the driven pile Dugan and Freed (1984).

- The horizontal movement of single piles in clay due to external soil displacements is comparable to the greenfield soil displacements given the inability of piles to resist displacements in its weak transversal direction (Chen and Poulos 1997).

- The horizontal movement of a foundation slab can be considered to be uniform over the stiff horizontal direction of the slab. When subjected to displacements, piles connected to the slab will thus have similar displacements at the pile head while being subjected to different magnitudes of displacements from the soil as a function of the distance from the source of displacements (Xu and Poulos 2001).

An additional remark is that existing foundations are not only subjected to, but also influence the distribution of soil displacements in a complex soil-structure interaction problem (Zhou et al. 2021). For piles subjected to external displacements, the emerging boundary conditions have a major impact on the predicted deformations in the pile. For an existing pile group, the boundary conditions for the single piles result from a system-level soil structure interaction.

3.3 Modelling of the pile cycle

Numerical modelling of the pile cycle in fine-grained soils, such as soft natural clay, involves capturing the kinematics from pile installation and the corresponding soil response. A number of modelling assumptions need to be made. Each assumption is associated with different degrees of simplification of the system response and, thus, influences the accuracy of the results.

Numerical methods

Table 3.1 presents some of the numerical methods previously used to investigate the impact of pile installation as part of geotechnical numerical analysis. The kinematics from the vertically installed pile can either be introduced with a vertical penetration (V) of the full pile length or, in a simplified approach, by a horizontal (H) numerical cavity expansion method (CEM). The CEM introduces the kinematics associated with the pile installation by a horizontal expansion of a predefined cavity (or volume element) equal to the length of the pile. The volume expansion of the cavity should be equal to the cross-sectional area per unit length of the pile.

Furthermore, the accuracy of different constitutive models for capturing the behaviour of natural clays, as described in Section 2.6, needs to be evaluated. Additionally, the drainage response in the soil can be captured by assuming an undrained (U) response in either a total stress (T) or an effective stress (E) formulation or by including the emerging coupled hydro-mechanical response (C).

Conventionally, the Finite Element Method (FEM) in geotechnics relies on a Total Lagrangian (TL) or an Updated Lagrangian (UL) numerical formulation. In TL the mesh used for spatial discretisation is fixed in space, so no change in the problem geometry is considered. In UL, the nodes of the mesh move with the calculated displacements and thus considers the updated geometry of the problem. In the case of modelling large deformations from pile installation, however, the updated mesh becomes severely distorted leading to numerical convergence issues. The Press-replace method (PRM) can be used to approximate a vertical pile installation using a conventional small-strain Lagrangian formulation. The pile installation is modelled by repeating sequences of press and replace steps. In the press step, a displacement boundary condition is used to press soil at the pile tip away, which is then replaced by pile material in the replace step.

To avoid convergence issues related to a distorted mesh, several different FEM formulations based on an Eulerian framework have been developed. An Eulerian formulation relies on a mesh that is fixed in space while the field variables, *i.e.*, stress, strain and state variables, are convected through the domain between calculation steps. The installation of a pile in an Eulerian formulation can be introduced by applying boundary conditions that mimic the penetration of a rigid pile.

A number of studies rely on a combination of the two formulations to overcome issues related to large deformations. The Arbitrary Lagrangian-Eulerian (ALE) formulation relies on a periodical re-meshing or reshaping of a deformed Lagrangian mesh by an Eulerian remapping of the field variables between the new and old mesh configurations. The Coupled Eulerian-Lagrangian (CEL) formulation instead divides the domain into a pure Lagrangian part and a pure Eulerian part. Contact formulations are introduced as boundary conditions in the relevant domains, and then the interaction between the two parts is specified.

Additionally, continuum-based particle methods, such as the Material Point Method (MPM),

Geotechnical Particle Finite Element Method (G-PFEM) and Smoothed Particle Hydrodynamics (SPH) can be used to model pile installation. These methods are conceptually comparable to the ALE methods, except that the field variables are tracked by convection of a number of predefined material points that move in space rather than being mapped between different mesh configurations.

In addition to FE methods, the analytical Cavity Expansion Method (CEM) and the Shallow Strain Path Method (SSPM) can be used to obtain the kinematics resulting from the pile installation, assuming a horizontal and vertical installation mechanism, respectively. The strain history, which is calculated independent of the soil response, from these two methods can then be combined with a constitutive model to get the change in the state of soil due to pile installation. A mapping from the single point response of the CEM or SSPM to an FE domain needs to be performed, if any continuum analysis, such as consolidation needs to be considered.

Numerical studies

Table 3.2 presents a number of numerical studies that influenced the modelling choices made in this Thesis.

The number of numerical studies that included the full pile cycle *i.e.*, installation, equalisation, and subsequent loading, of a displacement pile in a single numerical framework is scarce (Abu-Farsakh et al. 2015; Sivasithamparam et al. 2015a; Phek et al. 2023; Staubach et al. 2023). The influence of installation effects can be studied by comparing the load-displacement of a wished-in-place (WIP) pile with a numerically installed pile, see *e.g.*, Sivasithamparam et al. (2015a) and Staubach et al. (2023). The results indicate that the influence of pile installation is significant and increases with the introduction of strain softening in the modelled soil response (Sivasithamparam et al. 2015a) and with the number of load cycles (Staubach et al. 2023). The significance of strain-softening was also shown by *e.g.*, Hauser and Schweiger (2021) and Monforte et al. (2021), for the cone penetration test. The interplay between the rate-dependency and strain softening was highlighted by, *e.g.*, Zhou and Randolph (2009) and Singh et al. (2022) In conclusion, the above calls for a study on the combined influence of installation, rate-dependency and strain softening over all stages of the pile cycle.

The consolidation of positive excess pore water pressures results in a reduction in soil volume, which in combination with an increase in effective stress, leads to time-dependent increases in shear resistance. Additional compression of the clay occurs due to the ongoing creep in the soil. Furthermore, the destructured soil near the pile could regain some of the bonding of the *in-situ* soil due to thixotropy Ren et al. (2021). The phenomena are interlinked and are lumped together in the concept of pile ageing. Karlsson et al. (2019) studied the ageing using a rate-dependent soil response and concluded that the process of creep can be used as the major explanation for pile ageing. Pile ageing due to thixotropy has been included in numerical studies, *e.g.*, Abu-Farsakh et al. (2015) and Phek et al. (2023), by explicitly prescribing the strength properties of the disturbed clay. These studies do not include the influence of initial destructuration or rate dependency, and require a back-analysis of the time-dependent strength properties of the clay with calibration data. In the absence of full insight into the process of thixotropy, the process of ageing is in this work solely attributed to the influence of creep, which emerges from the intrinsic rate-dependency of the natural clay.

Numerical studies on soil displacements in clay resulting from both the pile installation stage

and the subsequent equalisation of excess pore water pressures are limited to CEM where the pile volume was introduced using a simplified horizontal pile installation mechanism (Castro and Karstunen 2010; Sheil et al. 2015). A direct comparison using FE between the displacement resulting from a simplified horizontal installation mechanism and that of a vertical installation mechanism is missing. This comparison should be performed to reveal the influence of this model assumption on the predicted displacements. Additionally, the relative influence of the features of soft natural clay on the emerging displacements due to pile installation and subsequent equalisation should be quantified.

Numerical studies of the full problem of pile installation tend to become computationally demanding. Simplifying the modelling process is sometimes necessary to study in detail the individual aspects of the impact of pile installation. An example is the quantification of the displacements resulting from a large number of piles installed in clay, which was studied by Edstam and Kullingsjö (2010) using a simplified numerical approach. The study relied on a constant volume response of linear elastic soil combined with a horizontal pile installation mechanism. The individual piles were grouped into a "superpile," which was the same length and equivalent volume as the individual piles. The method showed results comparable to SSPM and the measured field displacements, and is thus promising for assessing the influence of displacement on complex geotechnical systems in the short term.

Table 3.1: Numerical methods used for the numerical study of the pile cycle.

Method	Dir. [a)]	Soil [b)]	Stage [c)]	Example of user	Note
Two stage approaches					
SSPM + consol	V	EU, EC	I, C, L	Karlsson et al. (2019)	SSPM installation, FEM consolidation
CEM + consol	H	EU, EC	I, C, (L)	Randolph et al. (1979)	CEM installation, FEM consolidation
FEM- Small deformation					
1D CEM	H	EU (EC)	I,(C), (L)	Sivasithamparam and Castro (2020)	Horizontal expansion
2D CEM	H	EC	I, C, L	Abu-Farsakh et al. (2015)	Horizontal expansion + vertical shearing
3D CEM	H	EU, EC	I, C, L	Hoang et al. (2022)	Horizontal expansion
2D, flipped CEM	H	EU+EC	I,C	Sheil et al. (2015)	Horizontal plane
Press-replace method	V	EU, EC	I,C,L	Phek et al. (2023)	
FEM - Large deformation					
ALE Remeshing	V	TU (EC)	I, (C), (L)	Lu et al. (2004)	
ALE Reshaping	V	TU (EC	I, (C), (L)	Liyanapathirana (2009)	
Eulerian	V	EC	I, C, (L)	Dijkstra et al. (2011)	
CEL, uncoupled	V	EU+EC	I, C, (L)	Yi et al. (2021)	Switch between CEL (I) and UL(C)
CEL, coupled	V	EC	I, C, L	Staubach et al. (2023)	Full pile cycle + cyclic loading
Particle-based					
MPM	V	EC	I, C, (L)	Ceccato et al. (2016)	
G-PFEM	V	EC	I, C, (L)	Monforte et al. (2021)	
SPH	V	E(C)	I, (C), (L)	Cyril et al. (2022)	Coupled formulation in Bui et al. (2007)

[a)] Direction of installation: V=Vertical; H=Horizontal, [b)] E=effective stress, C=Coupled, U=Undrained, T=Total stress,
[c)] I = installation, C = Consolidation, L = Loading. Letter in () indicates the ability of the method,
but was not reported in the reference listed.

Table 3.2: Some relevant geotechnical applications of Finite Element Analysis to model effects of pile installation.

Reference	Method[a)]	Stage[b)]	Note
Sheil et al. (2015)	CEM H	I, C	Consolidation displacements, simplified 2D horizontal cross-section for pile group
Castro and Karstunen (2010)	CEM H	I, C	Consolidation displacements
Phek et al. (2023)	PRM V	I, C, L	Full cycle, explicit thixotropy to include ageing
Abu-Farsakh et al. (2015)	CEM H+V	I, C, L	Full cycle, explicit thixotropy to include ageing
Karlsson et al. (2019)	SSPM+FEM V	I,C,L	Creep is implicitly shown to explain ageing
Sivasithamparam et al. (2015a)	PRM V	I, C, L	Load-displacements for WIP vs installation
Staubach et al. (2023)	CEL V	I, C, L	Load-displacements for WIP vs installation, cyclic loading
Monforte et al. (2021)	G-PFEM V	I, C	Influence of strain-softening
Singh et al. (2022)	ALE V	I, C, L	Strain-softening, rate-dependent, consolidation, regain sensitivity
Edstam and Kullingsjö (2010)	CEM 3D H	I	Simple 3D analysis of displacements due to pile installation

[a)] Direction of installation: V=Vertical; H=Horizontal
[b)] I = installation, C = Consolidation, L = Loading.

4 Methodology development

4.1 Eulerian pile penetration

In this thesis, the Finite Element Method (FEM) formulation used to model the installation of piles into soft natural clays combines an Eulerian (E) material description for the clay with a quasi-Lagrangian description for the pile. The code used, Tochnog Professional (Roddeman 2024), has previously been used to model triggering and run-out of landslides (Crosta et al. 2003; Crosta et al. 2016) as well as pile installation (Dijkstra et al. 2011). In contrast to commonly used Total Lagrangian or Updated Lagrangian small strain FE codes, the formulation enables very large deformations around the tip of an advancing cone or displacement pile without numerical convergence issues.

The Eulerian description is based on the method suggested by Huetink (1992) where each time step is divided into an initial Updated Lagrangian step followed by the convection of material (and its state variables) through a stationary mesh with the Streamline Upwind Petrov Galerkin method (SUPG). The Finite Element mesh is fixed, *i.e.*, independent of the material deformations, throughout the analysis. However, at each time step any change in the geometry, *e.g.*, a second Lagrangian mesh or a geometry entity with prescribed boundary condition is continuously updated. A fully hydro-mechanically coupled numerical formulation with an effective stress-based constitutive model is used to couple the deformation of the material (volumetric and shear strains) to the emerging pore water pressure and flow of the pore water and vice versa. The hydraulic head in the system and the flow of pore water are computed with the storage equation, solved simultaneously with the mechanical problem for the ongoing pile penetration. Hence, the drainage response for each element in the domain will emerge from the hydraulic conductivity of the soil and the penetration rate of the pile. As a result, in addition to the undrained or drained penetration problem, intermediate drainage regimes spanning from undrained to drained response can be studied.

For an Eulerian mesh, two different methods to model the installation of a pile into the soil have been proposed by Dijkstra et al. (2011). Both rely on an Eulerian framework and an axisymmetric model domain but are fundamentally different in how the kinematics of the problem are introduced in the domain.

In the *fixed pile* method the problem is modelled as a stationary flow problem where the pile is fixed and the soil is flowing upwards in the domain. The pile geometry will affect the flow patterns in the soil, thus capturing the pile penetration mechanism. A steady state solution will eventually be reached for the specified geometry of the model.

A more intuitive way of modelling the penetration process is by the *moving pile* method, where pile installation is modelled by penetrating a pile object into an initially stationary soil. In this approach, the geometry of the pile and the boundary conditions prescribed on that entity, are gradually changed. As the pile is pushed further into the soil, the solution will show the current geometry at any given moment during the calculation. Analogously to modelling a flat pile base, another shape of the penetrating object can be used for both of these methods.

Fixed pile

The *fixed pile* method considers a pile with a radius R that is initially embedded to the full penetration length L of the pile at the axisymmetric boundary in a homogeneous soil , see Figure 4.1. The geometry is kept constant throughout the analysis. The kinematics of the method are introduced by a vertical inflow v of soil (and its state variables) at the bottom boundary of the domain. Pushing the soil already in the domain up and eventually out of the domain at the top boundary. As the soil continuously flows upwards, the stationary pile affects the flow pattern of the soil, and the penetration mechanism of the pile installation is modelled. Eventually, a steady state is reached, giving a solution to the problem for the specified geometry. Due to the flow of soil in the domain, the *fixed pile* method is limited to a homogeneous initial stress state in the soil. In the analysis, the soil can be modelled as a fluid, but more commonly, an effective stress-based constitutive model developed for soils is used. This initial stress state is prescribed through the domain, and in equilibrium in between the vertical force q applied as a boundary condition at the top of the domain and the inflow. Soil entering the domain through the bottom boundary is prescribed the initial stress state throughout the calculation.

Numerically, the pile is included by adjusting the geometry of the axisymmetric boundary to the shape of the pile, though a pile material can also be added. Two different ways of applying the boundary conditions (BC) from the pile geometry on the soil will be used (Figure 4.1). The fully fixed BC prevents all movement at the nodes in the soil that are connected to the pile. In contrast, the fixed normal BC only prevents nodes from moving in the normal direction to the pile geometry. Below the pile, regular axisymmetric boundary conditions are used to prevent horizontal displacements. Horizontal displacements are also set to zero at the far-right boundary.

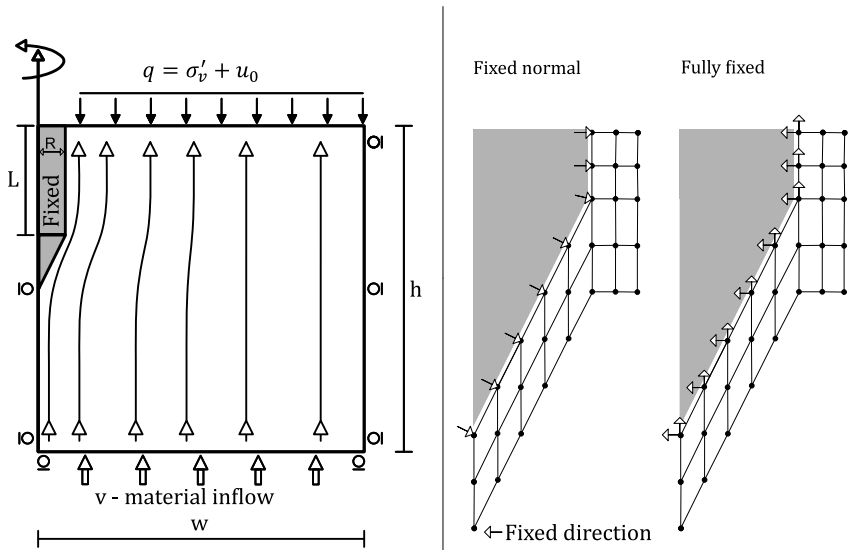

Figure 4.1: *Fixed pile method. Boundary conditions between the soil and the pile can either be modelled as fully fixed or fixed only in the normal direction.*

Moving pile

The second method for modelling pile installation, the *moving pile* method is illustrated in Figure 4.2. In contrast to the *fixed pile* method, the pile is initially located above the axisymmetric domain. The pile is modelled with a geometric entity to help mapping the boundary conditions on the nodes. Here, a quadrilateral with radius R, is defined to represent the pile initially outside the domain. Penetration is modelled by moving the bottom line (two nodes) of the quadrilateral, which represents the pile, downwards with a velocity v representing the penetration rate into the soil. As the pile geometry continuously expands downwards, a mapping is performed at each time step to check which of the nodes in the domain are at the location of the pile geometry. All nodes within and on the boundary of the pile geometry will be given a vertical velocity equal to the penetration velocity of the pile, while the horizontal velocity is set to zero. This process is repeated until the pile geometry has reached the final penetration depth L. Once all nodes of an element are associated with the pile geometry, the element can either be deleted or prescribed with a material for the pile. Both of these choices will lead to a completely rigid pile during the installation stage, *i.e.*, all nodes have a prescribed velocity. In this modelling approach, all the steps in between the initial and final calculation steps represent a valid solution for the specific geometry of the current time step.

At the left and right vertical boundaries, the horizontal displacements are fixed. Initially, before the pile enters the domain the initial stress state of the model is set. In addition to the possibility of prescribing a homogeneous stress state in equilibrium with the vertical load q on the top boundary and the bottom boundary, as in the case of the *fixed pile* method, also a more natural gravity based stress distribution can be calculated in an initial step.

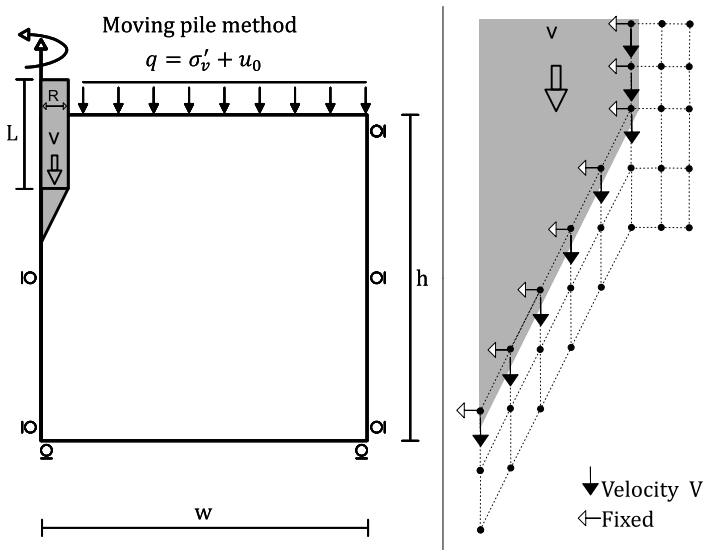

Figure 4.2: *Moving pile method.*

Verification

The numerical method used in this work was verified by investigating the penetration of a Cone Penetration Test (CPT) into the clay. To verify the modelling method, CPT is preferred over the flat pile geometry due to the large number of theoretical studies available on the problem of CPT penetration. In addition, an extensive empirical database is available on the relation between the soil properties and the response of CPT (Robertson 1990; Schneider et al. 2008).

Initially, the *moving pile* method and the *fixed pile* method were used to model the CPT geometry penetrating into a soil with a homogeneous stress state and soil properties. After reaching the final penetration depth, the two calculations have identical mesh and geometry. A linear elastic perfectly plastic stress-strain relation with the Tresca failure criterion was used to model the behaviour of the soil . A Poisson's ratio of $\nu = 0.49$ ensured a constant volume response, similar to the undrained response of saturated fine grained soils, such as clays. An uniform initial stress was set throughout the domain with vertical stress σ_v =5 kPa and a lateral earth pressure coefficient at rest K_0 equal to 1. For the first set of simulations, a Young's modulus $E = 5960$ kPa combined with a shear strength s_u of 40 kPa was used with a rough interface.

Figure 4.3 shows the resulting vertical penetration resistance on the tip of the CPT from the *moving pile* method and the *fixed pile* method using two different boundary conditions. The *moving pile* method and the *fixed pile* method with fully fixed boundaries show very similar results. The penetration resistance was found to be within 2% when comparing the two simulations.

The fixed pile method, in combination with BC that prevents displacements in the normal direction, initially indicated a considerably lower resistance However, this is a numerical artefact. The difference can be explained by studying the application of BC in Figure 4.1. The node located at the shoulder of CPT, at R is in the formulation using a normal boundary condition allowed it to move freely along the CPT. In contrast, the fixed boundary condition forces the soil closest to the CPT, at R, to be stationary. Hence, a displacement will occur in the node located one element width away from the pile geometry which results in a numerical extension of the radius. Since the model is axisymmetric, a rather small increase in the radius leads to a large increase in the area and the corresponding vertical force. The results included in Figure 4.1 correct for this fictive radius extension, and agree well with the other results.

Furthermore, the numerical method was also compared with prior numerical studies from literature on the resulting cone resistance on a CPT tip penetrating into a Tresca material. The *fixed pile* method with fully fixed boundary conditions was used and the resulting cone factor was calculated from a series of simulations using different rigidity index $Ir = E/s_u$. The cone factor is calculated as the resistance of the cone tip over the undrained shear strength of the soil. All other model parameters are kept constant throughout the series of simulations. Table 4.1 shows the computed cone factor for both smooth and rough contact formulation. The results are compared with a range of cone factors from previous studies summarised in Liyanapathirana (2009). For the smooth interface formulation, the results correspond to the upper range of the literature, whereas the results for the rough interface are closer to the lower range found in literature. The results for both the smooth and rough interface from this study show a similar dependency on the rigidity index as the previous studies.

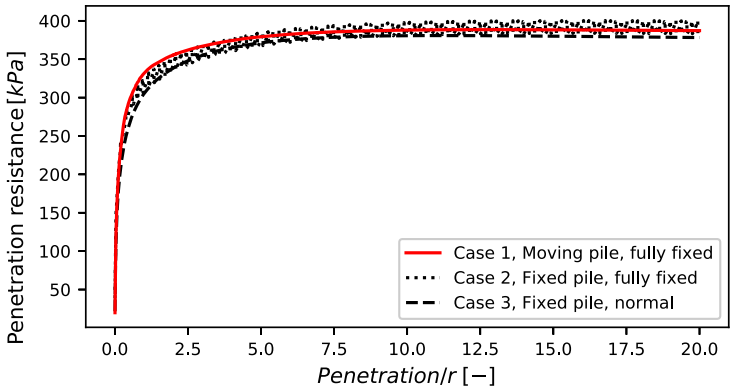

Figure 4.3: *Cone tip resistance from simulations using the fixed pile method with two different ways of applying BC and the moving pile method. Results obtained using* $E/c_u = 150$

Table 4.1: Simulated cone factor for different values of the rigidity index Ir. Data on previous studies from (Liyanapathirana 2009).

Ir	Contact	This study	Previous studies
50	smooth	8.6	8.1 - 9.6
	rough	9.3	9.4 - 13.8
150	smooth	11.5	9.8 - 11.4
	rough	12.2	11.8 - 15.0
300	smooth	13.2	10.6 - 12.5
	rough	13.9	13.3 - 15.8
500	smooth	14.1	11.2 - 14.4
	rough	14.9	14.4 - 20.7

Hence, the proposed numerical framework was shown to give results in accordance with previous studies. In addition, the two proposed methods for modelling the pile installation gave similar responses on the resulting tip resistance in the soil. As the *moving pile* method allows for a wider range of geotechnical applications, *e.g.*, linear increasing gravity loads, staged construction and intermediate calculation results, this method is preferred over the fixed pile method and was used for the rest of the simulations in this work. Furthermore, the *moving pile* method can be expanded to study multiple piles in a group in a 3D calculation.

4.2 Simulation of pile installation in soft clay

4.2.1 Comparison with physical model test

First, the *moving pile* method was used to model the physical model test conducted by Ni et al. (2010). The model test comprises a stainless steel pile with radius R of 4 mm being pushed down with length $L = 10R$ into an artificial soil created from mixing amorphous silica powder with two mineral oils. The artificial soil allows for determination of a cross-section of a 3D displacement field without wall effects affecting the results. Oedometer results of the transparent soil were reported, and the results were used to derive the MCC model parameters presented in Table 4.2. For the simulations, the *moving pile* method was combined with the hydro-mechanically coupled effective stress-based formulation with MCC to simulate the physical model test specified in Table 4.2. The size of the axisymmetric model is identical to the side of the laboratory domain face for which the displacements in the soil have been reported. The numerical model and mesh layout are similar to the model presented in Figure 4.6 and only scaled with the radius of the pile. The displacements from the numerical model are presented in Figure 4.4 together with the measurements from the physical model test. The vertical displacement contours are comparable between the simulations and laboratory tests, both with respect to the magnitudes of the displacements and the separation between the upward and downward displacements. The trend showing lower radial displacement towards the surface is similar between the simulations and model test. The magnitude of displacements is, however, significantly lower in the physical model test. The physical model test is conducted using a normalised penetration velocity of ≈ 7, which is slightly on the low side for an undrained system response and is thus in an intermediate drainage situation. Consequently, the system is very sensitive to small changes in stiffness and hydraulic properties that significantly influence the volumetric response upon loading. In conclusion, the comparison between the physical model test and numerical simulation shows that the *moving pile* method is able to capture the emerging displacements from the installation of a pile into clay.

Table 4.2: Input data for simulation of physical model test conducted by Ni et al. (2010).

e_0	κ	λ	M	ν	p_0 [kPa]	q[kPa]	k [m s^{-1}]
8.9	0.04	1.64	1.46	0.25	35	8	2×10^{-8}

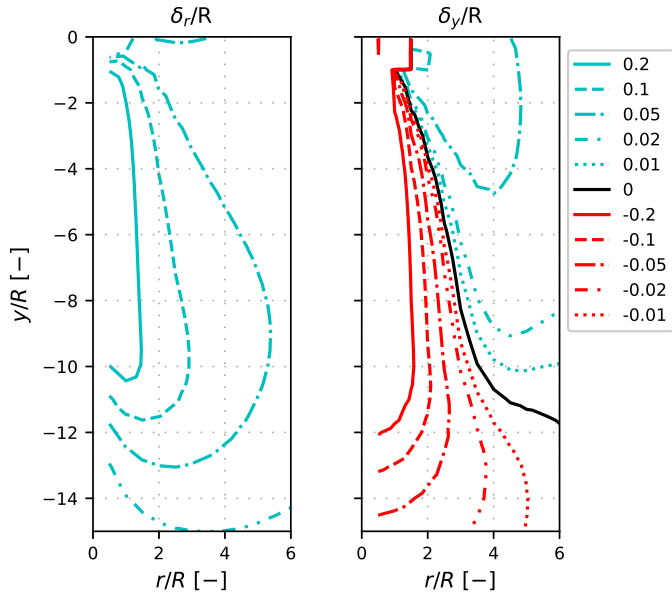

(a) *Simulation.*

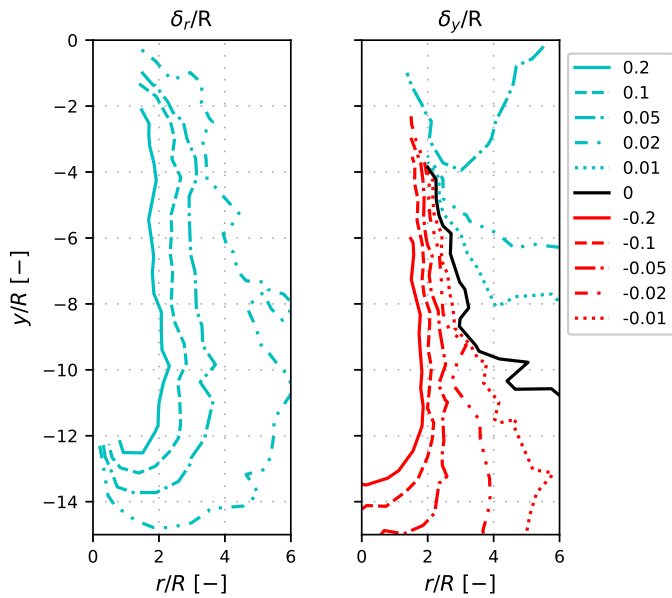

(b) *Physical model test.*

Figure 4.4: *Displacements due to the installation of pile with length* $10R$ *into an artificial transparent clay, comparison between simulations and physical model tests by Ni et al. (2010).*

4.2.2 Displacements due to pile installation in a natural clay

This section will present the simulated displacements due to the installation of a displacement pile into a soft natural clay. A numerical investigation on the influence of natural soft soil features will be conducted by presenting displacements when gradually accounting for the features of anisotropy, bonding, rate-dependency (creep) and small strains. This will be performed using the family of SCLAY models presented in Table 4.3.

Table 4.3: Soft natural clay features included in the constitutive models of the SCLAY model family.

Constitutive model	Anisotropy	Bonding	Creep	Small strains
MCC (MCC)	-	-	-	-
SCLAY1 (SC1)	x	-	-	-
SCLAY1S(SC1S)	x	x	-	-
Creep-SCLAY1S (CSC1S)	x	x	x	-
Creep-SCLAY1Sss (CSC1S-ss)	x	x	x	x

The properties of the modelled soft natural clay are based on the clay from the Utby test site, located east of Gothenburg on the west coast of Sweden. The clay deposit in Utby is approximately 30 m deep and on top of a 1 m to 3 m thick till layer on top of the bedrock. The soil properties determined from routine laboratory tests are presented in Table 4.4 and the results from a series of laboratory tests on the Utby clay can be found in Karlsson et al. (2016), including CRS test, IL test as well as anisotropically consolidated undrained triaxial tests sheared in compression and extension. Combined these tests allow for the calibration of the constitutive models.

The behaviour of the soft natural clay in Utby is modelled using the SCLAY1S and Creep-SCLAY1S constitutive models with the model parameters presented in Table 4.5. The small strain parameters were obtained from Tahershamsi et al. (2023) in the absence of relevant test data from the Utby site. The SCLAY1S model parameters are identical to the parameters derived for the Creep-SCLAY1S model by Karstunen and Amavasai (2017) and using λ_i and κ instead of λ_i^* and κ^* and simply excluding the parameters related to creep. The calibrated model response in undrained triaxial compression and extension loading path is presented in Figure 4.5 together with laboratory data.

Table 4.4: Index properties of Utby clay: wet density ρ, water content at plastic limit w_p, natural water content w_n, water content at liquid limit w_L, plasticity index I_p, sensitivity S_t and the undrained shear strength from fall cone test τ_{fu}. Data from Karlsson et al. (2016).

Depth [m]	ρ [t/m^3]	w_p [%]	w_n [%]	w_L [%]	I_p [%]	S_t	τ_{fu} [kPa]
5	1.55	25	81	63	38	30	10
6	1.59	22	71	55	33	26	9
7	1.58	20	72	55	35	27	10
8	1.54	23	71	60	37	28	14
9	1.58	19	75	61	42	29	17

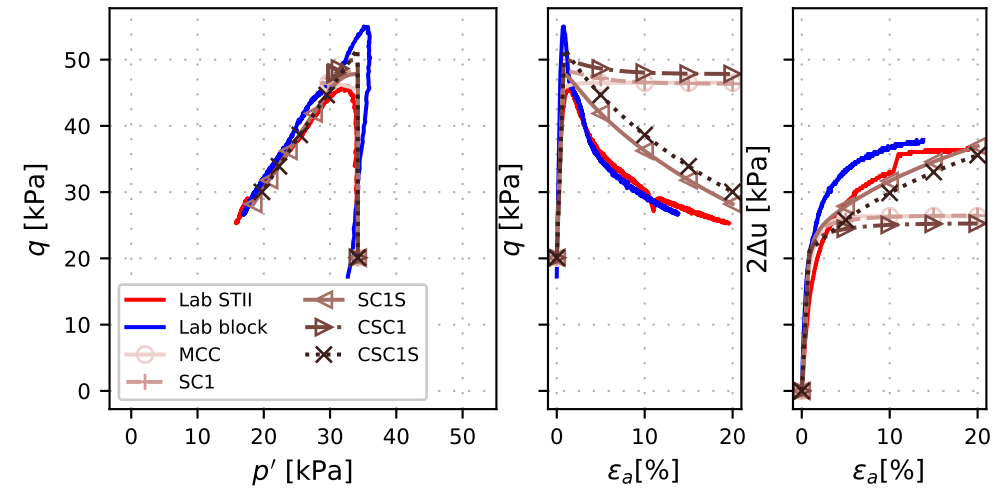

(a) *Compression.*

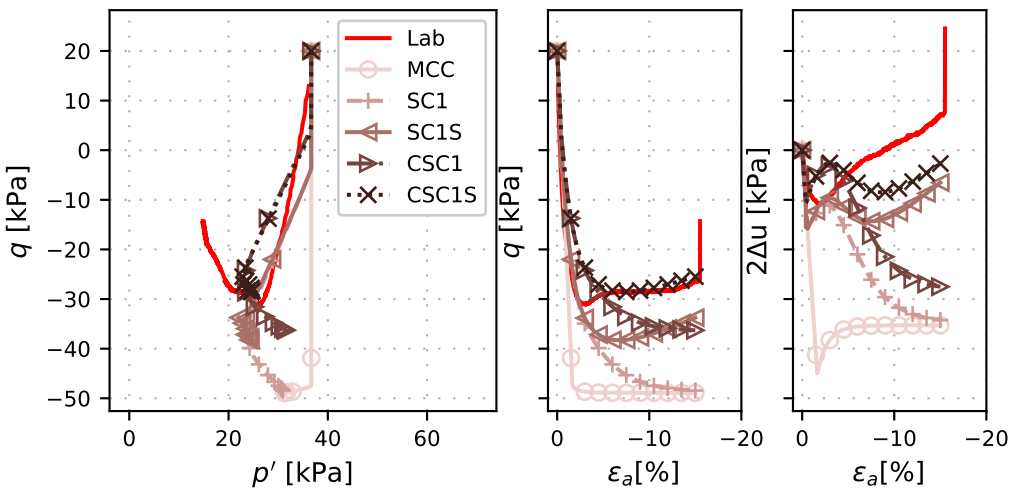

(b) *Extension.*

Figure 4.5: *Anisotropically consolidated triaxial testing of Utby clay. Laboratory data and calibrated response of the SCLAY model family.*

Table 4.5: Model parameters used for the coupled simulation of pile installation into Utby clay using SCLAY1S. From Karstunen and Amavasai (2017). Small strain parameters from Tahershamsi et al. (2023).

Symbol	Parameter	Value
K_0	Initial lateral earth pressure coefficient [-]	0.6
OCR	Overconsolidation ratio [-]	1.45
k	Hydraulic conductivity [m/s]	6.67 e-6 (1 e-9)
σ_v	Overburden load	18 kPa
ρ	Density	1.6 t m^{-3}
e_0	Initial void ratio [-]	2.05
κ^*	Modified swelling index [-]	0.02
λ_i^*	Modified intrinsic compression index [-]	0.108
λ^*	Modified compression index [-]	0.296
ν'	Poisson's ratio	0.2
M_c	Slope of CSL line in compression [-]	1.56
M_e	Slope of CSL line in extension [-]	1.15
α_0	Initial anisotropy [-]	0.63
ω	Rate of rotation [-]	30
ω_d	Rate of rotation due to deviator strain [-]	1.0
χ_0	Initial amount of bonding [-]	5
a	Rate of destructuration [-]	9
b	Rate of destructuration due to to deviator strain [-]	0.4
μ_i^*	Modified intrinsic creep index	0.00142
τ	Reference time	1 d
ϖ	Small strain multiplier	8
A	Shape factor for small strain stiffness degradation	0.005

The modelling was performed using the fully coupled deformation and pore water pressure formulation in Tochnog Professional (Roddeman 2024) in combination with the *moving pile* method. The left and right boundaries are modelled as roller boundaries, fixed in the horizontal direction, preventing any material displacements and groundwater flow, while the top boundary is modelled using a prescribed total vertical stress σ_v corresponding to the weight of the dry crust found on the Utby site, see Figure 4.6. Gravity is included in the analysis, which increases vertical stress (and hence stiffness and strength) with depth. The initial horizontal stresses are prescribed using the vertical effective stress and the earth pressure coefficient at rest K_0 equal to 0.6. The initial pore water pressures in the soil are set as hydrostatic pressures with a phreatic level at the top of the domain. The pile is modelled with a radius R of 0.155 m and is being pushed towards a final depth, corresponding to a pile length L, of $40R$ with a penetration rate v of 0.155 m s^{-1}. After installation of the pile into the soil, the pile is kept in place, and the excess pore water pressures are allowed to dissipate whilst monitoring the displacements in the soil. The width w is equal to twice the pile length, *i.e.*, $80R$ and the height h is equal to six times the pile length, *i.e.*, $240R$. The width and height of the domain were decided after a convergence study on the surface displacements

at a distance of two L from the installed pile. The influence of domain size is significant and elaborated on in Isaksson et al. (2025a) (see, Figure 7).

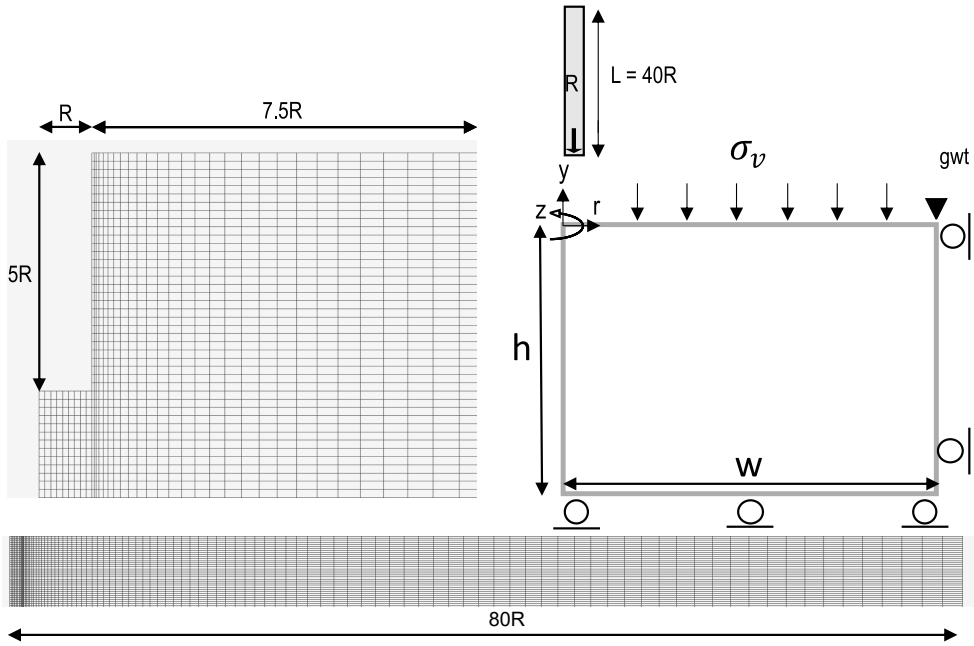

Figure 4.6: *Numerical model used to model pile penetration into Utby Clay.*

For the numerical analysis, the hydraulic conductivity k had to be increased compared to the *in-situ* value to avoid convergence issues resulting from a required minimum critical time step for coupled analysis, see, *e.g.*, Vermeer and Verruijt (1981). The minimum critical time step increases with the decrease in k and decreases with the decrease in element size. For the very low *in-situ* k, the required minimum time step was too large for an accurate solution with respect to the penetration velocity of the pile in relation to the element size. Another possible solution would be to reduce the minimum required time step by reducing the element size. However, this solution would increase the domain size considerably and result in very long simulation times. Although the time of consolidation will need to be scaled accordingly to match the *in situ* conditions, the pile penetration will still be modelled under practically undrained conditions, *i.e.*, in the analysis the normalised penetration rate V is ≈ 800, well above what is considered to fulfil penetration under undrained conditions ($V > 30$) (Schneider et al. 2007; DeJong and Randolph 2012; Mahmoodzadeh and Randolph 2014).

The Eulerian formulation of the numerical framework has a fixed mesh and solves for the velocity field (and displacements) in an Eulerian reference frame. Hence, special consideration was needed to extract the Lagrangian displacements of the soil caused by the pile installation. To get the displacements, 1614 discrete post points were defined in the domain. During the simulation, the post points were convected with the material flow using the velocity field in the domain. Therefore,

the position of a post point at any given time step can be interpreted as the displaced position of a soil element initially located at the respective post points in their original position.

The simulated displacement paths for four shallow ($1R$) soil particles and four mid-pile ($19R$) soil particles for the five different constitutive models are presented in Figure 4.7 and Figure 4.8 respectively. Generally, the shallow soil shows larger vertical and lower radial displacements compared to the deeper soil. The displacement directly after installation is quite uniform for all modelled soils. However, a difference is noticeable when introducing the features of anisotropy, sensitivity, and small strains, which result in a gradual increase in vertical displacements. The consolidation movement is strongly influenced by the feature of bonding. The simulations that consider bonding and destructuration show a significantly softer response compared to the models that do not.

In addition to the displacement paths of soil particles, the displacement of the soil in four vertical cross sections at a distance of $3R$, $10R$, $20R$, and $40R$ from the installed pile directly after installation and after full consolidation are computed. The radial displacements are presented in Figure 4.9 and the vertical displacements in Figure 4.10. A surface effect is evident, close to the pile at $3R$; the radial displacements are lower toward the surface while the vertical displacements are higher. The radial movement after pile installation is similar for clays at all distances from the pile. The small strain feature results in the lowest radial displacements and highest vertical displacements, which indicates that the horizontal stiffness gradient in the small strain simulation significantly impacts the displacement field by concentrating the soil movement closer to the pile. The features of bonding again strongly influence the movement due to consolidation.

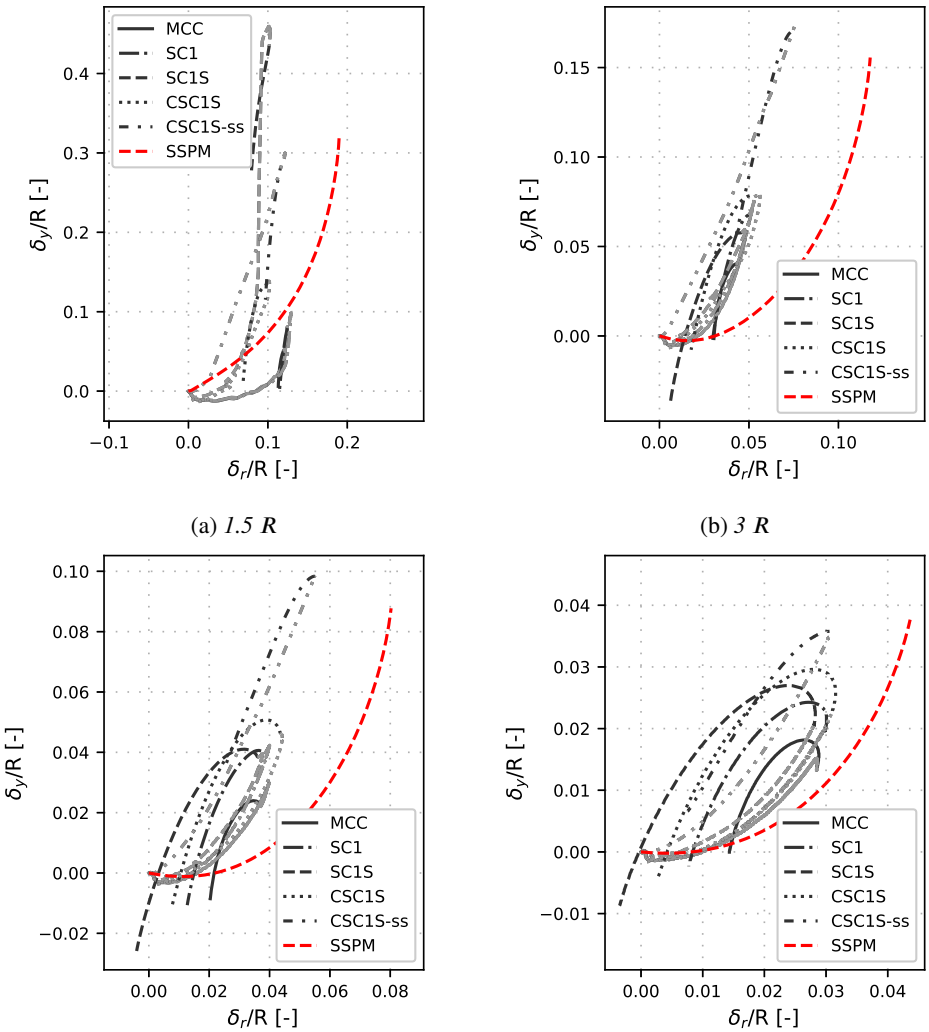

(a) *1.5 R*

(b) *3 R*

(c) *5 R*

(d) *10 R*

Figure 4.7: *Numerical displacement paths at different radial distances from the centre of the pile (*1.5R*,* 3R*,* 5R *and* 10R*) at a depth of* 1R *due to pile installation (light) and subsequent consolidation (dark). Influence of soft natural clay features indicated by including results from all constitutive models from Table 4.3. Displacements are normalised with the pile radius* R*.*

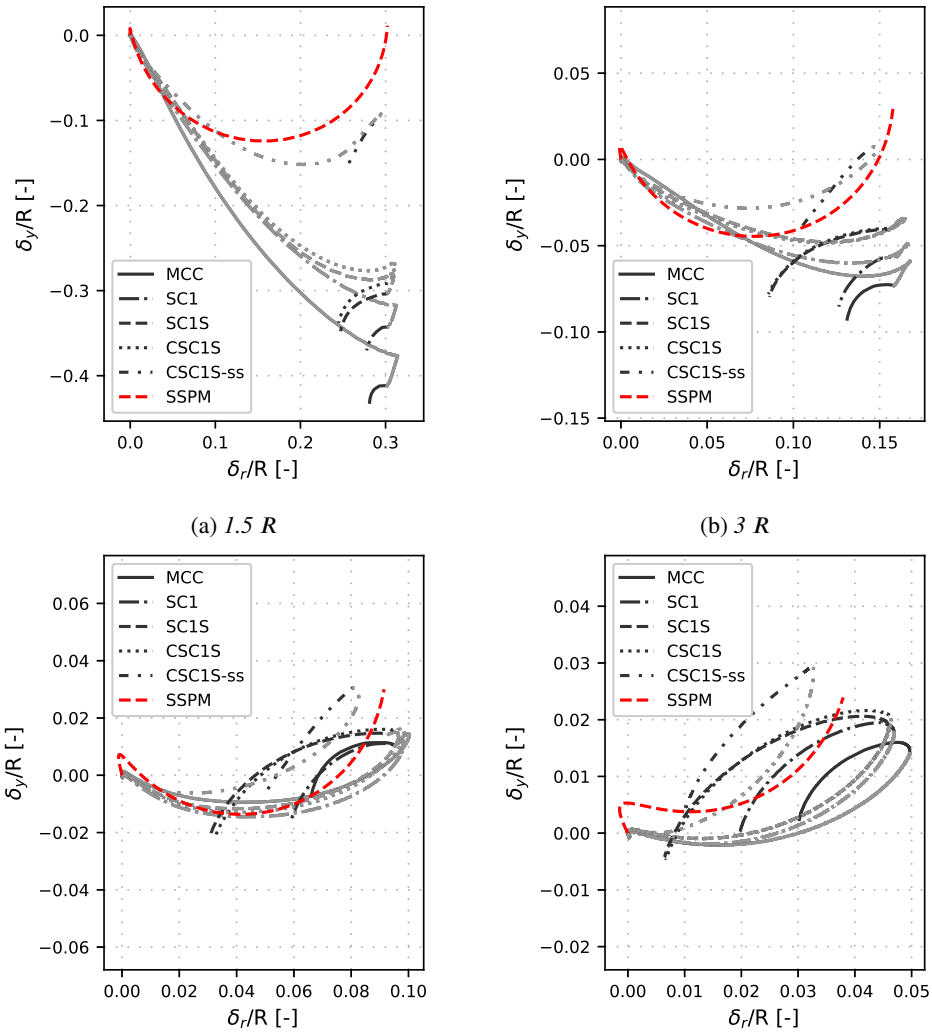

(a) *1.5 R*

(b) *3 R*

(c) *5 R*

(d) *10 R*

Figure 4.8: *Numerical displacement paths at different radial distances from the centre of the pile (*1.5*R*, 3*R*, 5*R and* 10*R) at a depth of* 19*R due to pile installation (light) and subsequent consolidation (dark). Influence of soft natural clay features indicated by including results from all constitutive models from Table 4.3. Displacements are normalised with the pile radius R.*

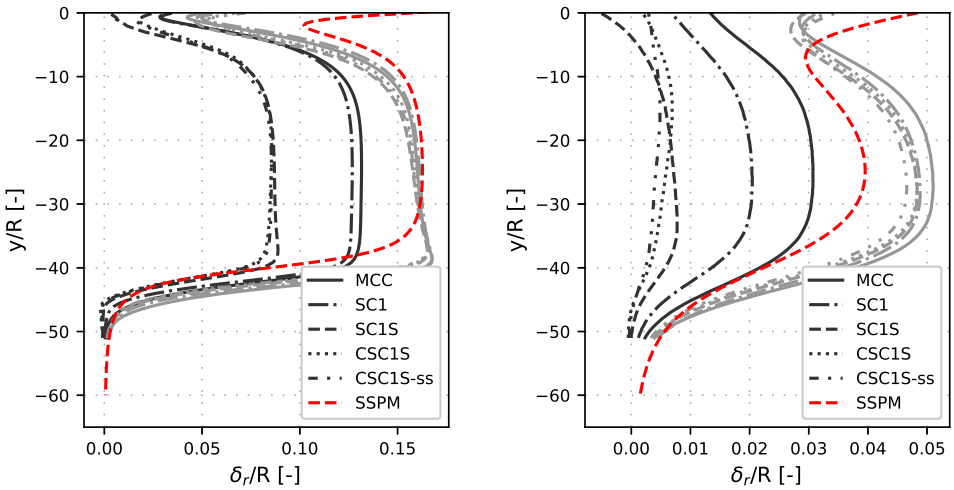

(a) *3R*

(b) *10R*

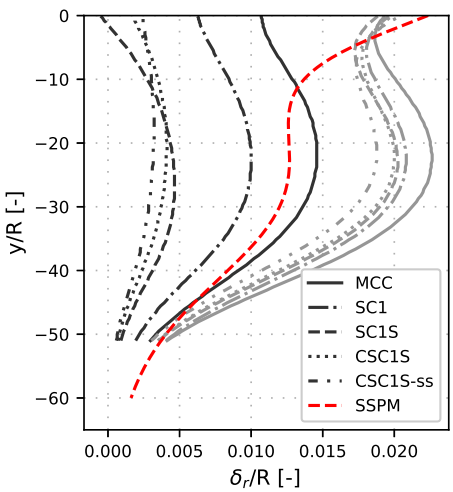

(c) *20R*

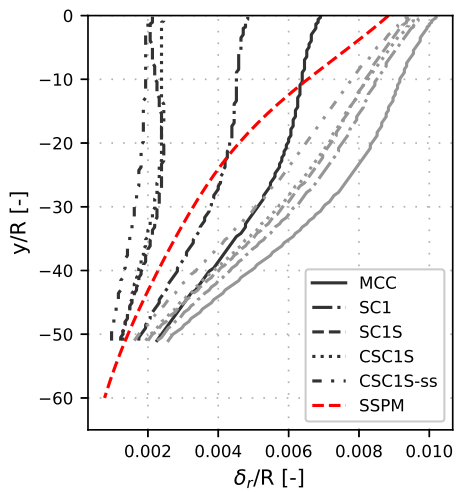

(d) *40R*

Figure 4.9: *Radial displacement from pile installation (light) and subsequent consolidation (dark) for four inclinometers (vertical cross sections) located at a radial distance of respectively 3R, 10R, 20R, and 40R. Influence of soft natural clay features indicated by including results from all constitutive models from Table 4.3.*

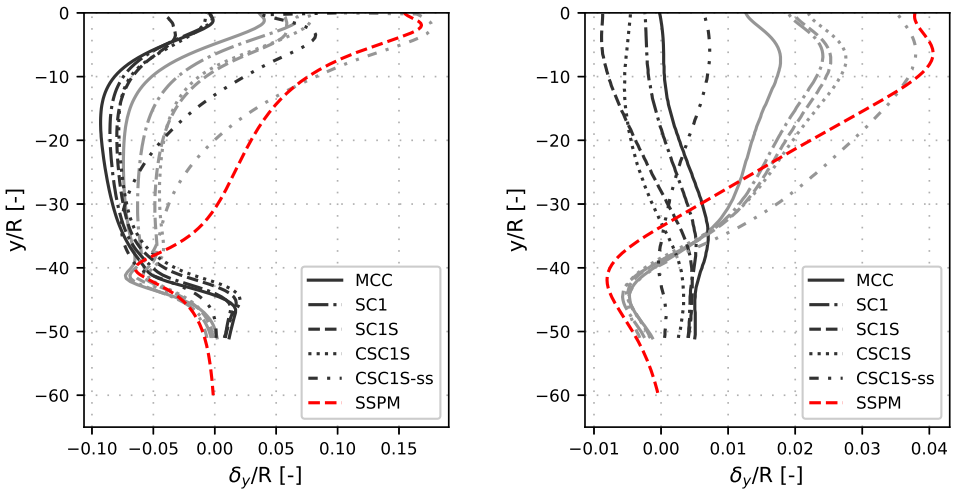

(a) *3 R*

(b) *10 R*

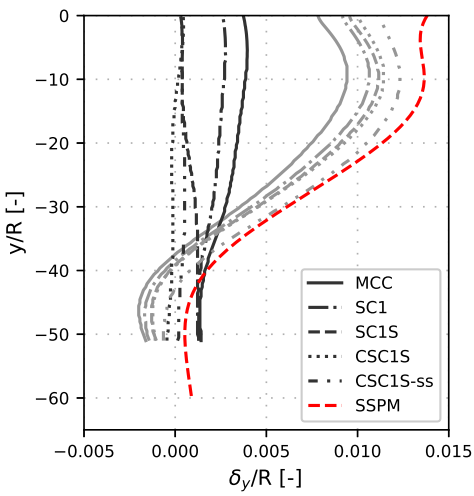

(c) *20 R*

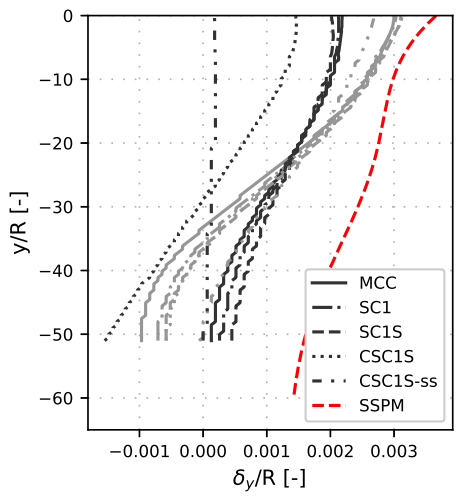

(d) *40 R*

Figure 4.10: *Vertical displacement from pile installation (light) and subsequent consolidation (dark) for four inclinometers (vertical cross sections) located at a radial distance of respectively 3R, 10R, 20R, and 40R. Influence of soft natural clay features indicated by including results from all constitutive models from Table 4.3.*

4.2.3 Global Sensitivity Analysis

In addition to investigating the emerging response by changing the constitutive model, a Global Sensitivity Analysis (GSA) was performed using SCLAY1S to discover the most important parameters influencing the emerging mass-displacements from the installation of displacement pile in an anisotropic sensitive clay.

The amount of site investigation data available from a geotechnical site is very limited in comparison to the volume of soil in the ground at the site. In addition, as a soil deposit is formed by nature, some variability of the material is expected (Phoon and Kulhawy 1999). Uncertainties from the limited site investigation are inherited by the numerical idealisation. A number of methods exist to quantify the impact of the anticipated uncertainties and to highlight the most important factors governing the model response.

Experimental design is a concept using a systematic approach of conducting Sensitivity Analysis (SA), aiming to provide the maximum possible information from a limited number of experiments (Box and Draper 2006). Experiments herein are referred to as the realisation of a numerical simulation with a specific set of parameters. Experimental design using the two-level factorial design is a statistical method in which the factors are given a low (-) and a high (+) value leading to a total of 2^k possible realisations for the full set of parameter combinations.

The realisation of the full set gives information about the main effects related to the change of a single parameter, as well as all possible interaction effects between two or more parameters. A fractional factorial design of resolution IV relies on the assumption that the interaction effects are small in comparison to the main effects. However, by assuming that the higher order interaction effects are negligible compared to the lower order interaction effects and the main effects, only a fraction of the full set of possible experiments needs to be conducted. The main effects for the change in a single parameter will with resolution IV not be confounded with any other main or two-factor effects.

Tahershamsi and Dijkstra (2022) conducted Global Sensitivity Analyses (GSA) using a numerical constant rate of strain oedometer test (CRS) on the impact of Creep-SCLAY1S parameters. The study highlights the importance of different parameters in the constitutive model at different temporal and spatial locations. The GSA was performed by means of Experimental design and the Sobol method to analyse the impact of different factors on the response of the CRS test. It was concluded that the effects of these factors change at different temporal stages of the CRS test, which correspond to the elastic and plastic response of the numerical model. The rational framework developed for GSA was also used in the studies conducted in this work.

The parameters and ranges considered in the SA are presented in Table 4.6. The - and + values represent a variation of $+-10\,\%$ from the mean. The Experimental design was chosen as a resolution IV fractional factorial design giving in total $2^{8-4}_{IV} = 16$ realisations. The choice of using a level IV resolution instead of the full factorial design reduces the number of simulations from 256 to 16. The combination of low and high values of the analysis for the 16 simulations is presented in Table 4.7.

The response will be quantified as the volume of soil normalised with the installed pile volume that is passing through the vertical cross sections presented in Figure 4.9. Figure 4.11 shows the GSA results for four vertical cross sections at a distance of ($3R$, $10R$, $20R$ and $40R$). The response is

Table 4.6: Range of parameters used in the two level fractional factorial sensitivity analysis for the modelling of pile installation into a sensitive anisotropic clay (SCLAY1S).

Parameter	Mean	-	+
κ	0.02	0.018	0.022
λ_i	0.108	0.0972	0.1188
χ_0	5	4.5	5.5
ω	30	27	33
a	9	8.1	9.9
b	0.4	0.36	0.44
OCR	1.45	1.305	1.595
M_c	1.56	1.404	1.716

Table 4.7: Table of contrast presenting the combination of parameters used for the 16 analyses needed for the two level fractional factorial experimental design 2^{8-4}_{IV} sensitivity analysis.

Run no.	κ	λ_i	χ_0	ω	a	b	OCR	M
1	-	-	-	-	-	-	-	+
2	+	-	-	-	+	+	-	-
3	-	+	-	-	+	-	+	-
4	+	+	-	-	-	+	+	+
5	-	-	+	-	-	+	+	-
6	+	-	+	-	+	-	+	+
7	-	+	+	-	+	+	-	+
8	+	+	+	-	-	-	-	-
9	-	-	-	+	+	+	+	-
10	+	-	-	+	-	-	+	+
11	-	+	-	+	-	+	-	+
12	+	+	-	+	+	-	-	-
13	-	-	+	+	+	-	-	+
14	+	-	+	+	-	+	-	-
15	-	+	+	+	-	-	+	-
16	+	+	+	+	+	+	+	+

analysed both directly after installation (I) and after consolidation (C). The effect, *i.e.*, change in response from changing each parameter from the min to max value, is normalised with the sum of the absolute effect for all the realisations. A negative response indicates that the total volume of soil passing through a cross-section is decreased when the specific parameter is changed from the - value to the + value. The total effect and the mean response are included at the top of the figures. A general trend for all of the analyses worth highlighting is that the total effect is low after installation compared to the total effect after consolidation. This indicates that the impact of the soil properties and the parameters controlling those is strongly increasing after effective stresses start changing during the consolidation in the soil. The most influential parameters on the displacements after consolidation are κ, λ_i, OCR and M.

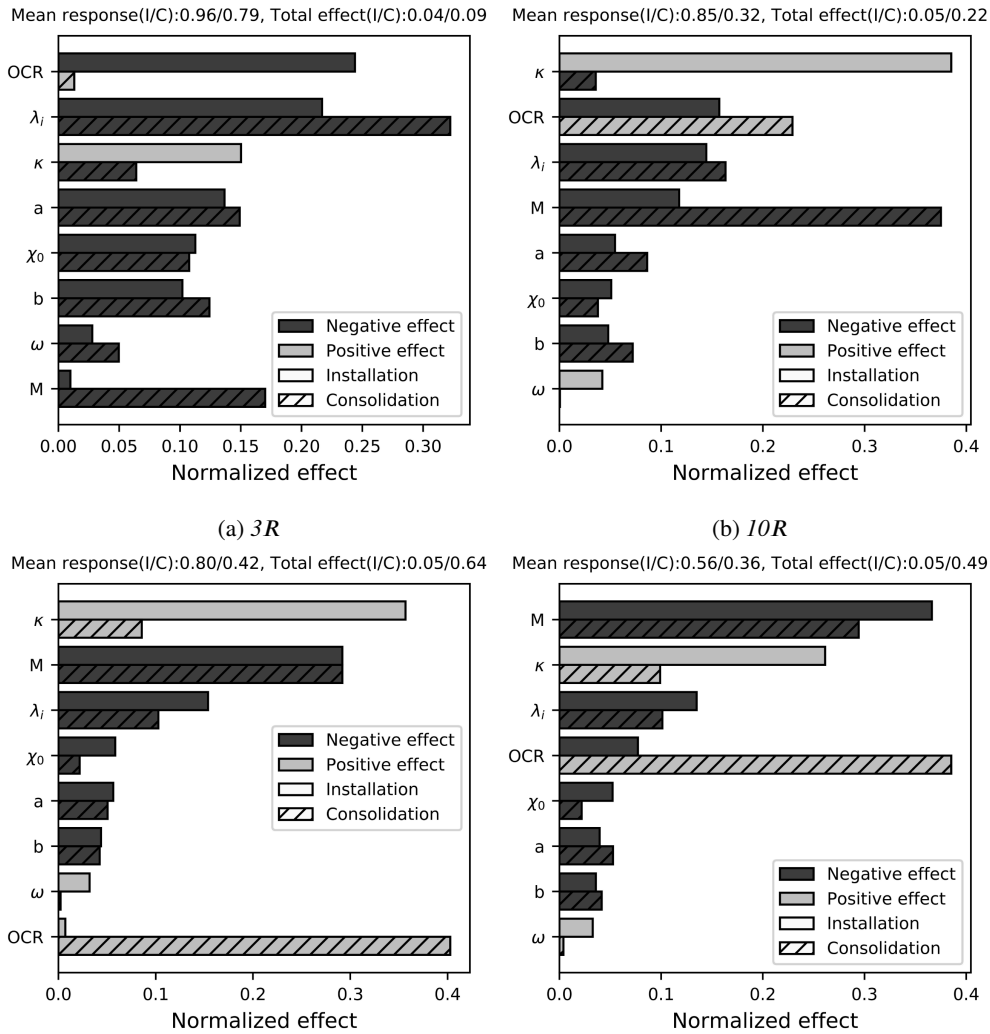

(a) *3R* (b) *10R*

(c) *20R* (d) *40R*

Figure 4.11: *Relative effect of model parameters on the mass displacement from piling in an anisotropic sensitive clay captured with the SCLAY1S model.*

5 Research summary

5.1 Overview of methodology

The research aims to quantify the effects of installing displacement piles in natural clay on the existing geotechnical system *in-situ*. The geotechnical system considered herein, contains the soft natural clay and its extent to stiff boundaries, as well as existing geotechnical structures already embedded in the clay. The resulting displacements and change in state result from the interaction between the kinematics induced by the pile installation process and the emerging response of the soft natural clay. The pile cycle (Randolph and Gourvenec 2011) is used as a conceptual model for the investigations conducted. Different numerical approaches with varying degrees of accuracy, *i.e.*, numerical framework and constitutive models, are used to quantify the effect of pile installation at different stages of the pile cycle. The complexity varies with respect to the *in-situ* conditions, the modelled soil response, and the methods used to simulate the kinematics of the installation of displacement piles. An overview of the work conducted in this thesis and the focus of each part is presented in Figure 5.1.

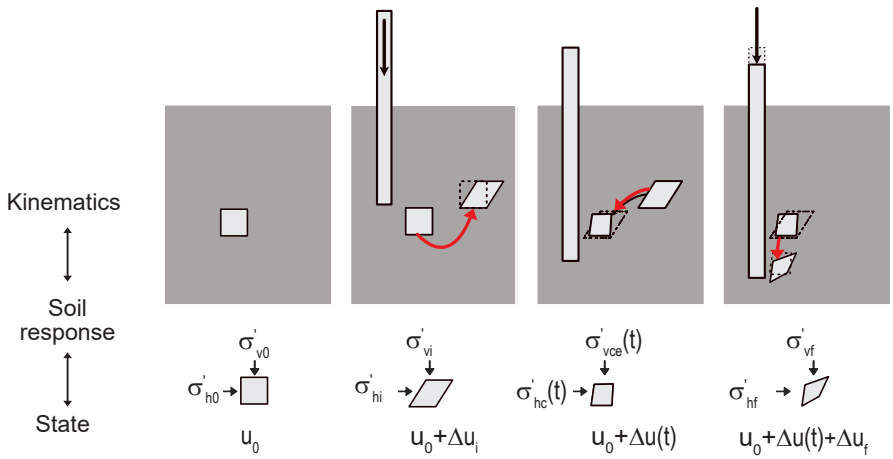

	In-Situ	Installation	Equalisation	Loading
Methodology development	Soil	Kinematics	Kinematics	
Paper A	Soil	State		
Paper B		State Kinematics	State Kinematics	
Paper C	Soil	State	State	State
Paper D	Soil	Kinematics	Kinematics	
Paper E	Foundation	Kinematics		
Paper F	Foundation Domain size	Kinematics		

Figure 5.1: *Outline of the methodology.*

The initial **methodology development** focuses on establishing an advanced numerical method for simulating the vertical penetration of a displacement pile into a soft natural clay. The method relies on an Eulerian numerical formulation to overcome the problems related to large deformations around the advancing pile base. The framework incorporates a coupled effective stress-based formulation using an advanced constitutive model. This first part focuses on quantifying the kinematics following the pile installation.

Paper A presents numerical simulations of CPTu using the advanced numerical method established. The purpose is to benchmark the coupled formulation and the advanced constitutive model used to capture the evolving state in the soil. The results are compared against the normalised penetration velocity framework and two empirical soil behaviour type charts.

Paper B focuses on capturing the evolving state and displacements in the soil surrounding the pile. The installation effects are investigated for different penetration rates, *i.e.*, emerging drainage conditions. The influence of the pile installation on the state of the soil is quantified using numerical triaxial tests conducted on the current state of the soil that is extracted at different stages of the simulated pile cycle.

Paper C demonstrates the ability for including pile installation in spatio-temporal system-level analysis. The ideal constitutive model for this analysis in geotechnical engineering should capture all potential loading situations for a specific soil element with a single consistent parameter set. The paper investigates the influence of common features of soft natural clays on the simulated response in different loading situations commonly experienced by the soil, including the triaxial test, oedometer test and CPTu. Additionally, the paper investigates the evolving spatio-temporal state and response of the pile-soil system over the installation, equalisation and loading stages of the pile cycle.

Paper D benchmarks simple and advanced methods for predicting the kinematics due to pile installation directly after installation and after consolidation. The methods are associated with varying model complexity, including the soil features modelled and the way of modelling the pile installation. The influence of the model fidelity in the modelling on the computed mass-displacements is discussed.

Paper E compromises a case study where the displacements from pile installation in clay are investigated with a focus on quantifying the influence of including the interactions of an existing foundation. This exploits the insights from previous model development, in which the kinematics from the installed piles are introduced by a simplified horizontal mechanism, and the soil is modelled as a linear elastic continuum. Structural elements are used to include the influence of the existing structures, and the results are compared with field data.

Paper F extends the work of **Paper E** by generalising the soil-structure interaction resulting from an existing deep foundation and the resulting displacements from the pile installation. The response of the system is quantified with respect to the displacement of the existing foundation. Additionally, the influence of pile spacing, foundation area, and relative stiffness between the structure and the soil is quantified. Finally, the influence of domain size on the distribution of displaced soil is highlighted.

5.2 Summary of the appended papers

Paper A: "Simulation of CPT penetration in sensitive clay"

Paper A compromises a numerical study of a CPTu test. The paper validates the coupled Eulerian numerical framework in combination with the constitutive model SCLAY1S. The CPTu response was investigated for the full range of drainage conditions, including the emerging drained and undrained limit states. The effect of the constitutive model was investigated by comparing the response of the numerical CPTu simulations with different soil models.

A brief summary of some key results and conclusions is provided in the following:

(i) Successful simulations combining an advanced constitutive model in an Eulerian coupled effective stress numerical framework were conducted.

(ii) The results show that the coupled formulation, in combination with the Eulerian numerical framework, is able to capture the emerging drainage conditions due to CPT penetration into clay. The transition from a drained to an intermediate and undrained system was quantified using the normalised penetration velocity. The response agrees well with previous laboratory and numerical studies.

(iii) The influence of the modelled soil features on the CPTu response was investigated using SCLAY1S. The influence on the response was compared to the expected response based on two common empirical Soil Behaviour Type charts (SBT). The influence of sensitivity and OCR are in accordance with the expected response based on SBT. The influence of the overconsolidation ratio and sensitivity was notable. The influence of anisotropy, as captured by SCLAY1S, was limited.

(iv) The study indicates a possible mutual benefit between numerical modelling and empirical SBT charts. The SBTs can be used as a benchmark for numerical frameworks, and the numerical methods can be used to link soft natural clay features to the response in SBT charts.

Paper B: "Modelling pile installation in soft natural clays"

Paper B presents a numerical study on the effect of pile installation on the displacement and state of the soil in the vicinity of a pile installed in soft natural clay. The installation effect is investigated for drained, intermediate and undrained pile installation. The state change is quantified using a numerical triaxial test on soil numerically extracted from the domain at different stages of the pile cycle. The modelled soil is based on a soft natural clay found in Utby, Gothenburg, Sweden.

A brief summary of some key results and conclusions is provided in the following:

(i) The displacements due to pile installation are strongly influenced by the emerging drainage conditions during pile installation. The vertical displacements within $1.5R$ from the installed pile are smallest for the undrained state and largest for the drained state, while the radial displacements are similar in magnitude for all drainage conditions. At a larger distance, the undrained situation shows considerably larger displacements than the intermediate and drained state. The drained displacements beyond a distance of $5R$ are very small.

(ii) The changes in state in the soil resulting from the pile installation are considerable. The structure of the soil has been severely modified, as indicated by the non-brittle isotropic response of the soil sampled from the disturbed zone, in relation to the brittle anisotropic response of the intact soil.

(iii) An undrained pile installation leads to a temporary reduction of the shear strength of the soil followed by a regain in strength following consolidation.

(iv) The installation of the pile with a rate that is in the drained regime, results in a higher shear strength in the soil compared to the original strength in the soil prior to installation.

(v) A K_0 consolidated triaxial test for soil extracted from the undrained pile installation after full consolidation results in considerably higher shear strengths compared to the response when the soil is tested at the stress state found in the numerical model. In contrast, no significant changes in the shear strength was found when the same investigation was performed on soil sampled close to the pile after the drained and intermediate pile installation.

Paper C: "Modeling the pile cycle of an axial loaded pile in sensitive natural clay"

Paper C presents the simulation of a pile test conducted in a soft marine clay following a field test conducted in Bothkennar, Scotland, reported by Lehane and Jardine (1994). The paper aims to investigate the possibility of using a single consistent parameter set calibrated against laboratory data to capture the system response over the full pile cycle. The numerical study compares the triaxial response, oedometer response in intact and reconstituted samples, and the CPTu response of the Bothkennar clay. The models used include the isotropic (MCC), anisotropic (SCLAY), anisotropic and structured (SCLAY1S), rate-dependent anisotropic (Creep-SCLAY1), and rate-dependent, anisotropic and structured (Creep-SCLAY1S) model versions. The full pile cycle is quantified using the Creep-SCLAY1S model, and the results are compared to those of commonly used design methods for pile capacity.

A brief summary of some key results and conclusions is provided in the following:

(i) The numerical CPTu response using MCC, SCLAY1 and Creep-SCAY1S is close to the measured response in the field. Creep-SCLAY1 overpredicts the net tip resistance and underpredicts the excess pore water pressures, while SCLAY1S underpredicts both the pore water pressures and tip resistance. This indicates that the effects of destructuration and rate-dependence are opposite and of equal magnitude, and hence seem to compensate for each other for simulation of CPTu penetration.

(ii) The only model that is able to capture the triaxial, remoulded and intact oedometric response and the CPTu is Creep-SCLAY1S. These loading situations are all representative of the soil response over the pile cycle in clay. Creep-CSLAY1S is thus considered the only model suitable to model the pile load test.

(iii) The numerical results show a good agreement with the general trends found in the pile load test. The influence of loading rate, set-up time and loading direction, as captured by the numerical simulations with Creep-SCLAY1S, agrees well with the trends from the field test. However, the magnitude of stresses is systematically lower in the numerical simulations, which is considered to be arising in the installation stage where pore water pressures are underpredicted. This underprediction then remains in the later stages of the pile cycle.

(iv) The results show that the numerical method is able to explain the gain in shaft capacity over time as seen in the field, both due to consolidation and due to creep (rate-dependency).

(v) The results highlight the strong influence of including the installation effect on the state of the soil, when using advanced constitutive models for geotechnical system analysis.

(vi) The paper corroborates the strong link between the CPTu results and the pile capacity, *e.g.*, the empirical relations proposed by Lehane et al. (2022).

(vii) The paper indicates that the testing and calibration of model parameters is challenging in the post-peak regime.

Paper D: "On modelling pile installation in soft natural clay. "

This manuscript includes but are not limited to the results presented in Section 4.2. The aim of the manuscript is to investigate several methods for modelling pile installation and their impact on the predicted mass-displacements directly after pile installation and after consolidation. In addition to benchmarking simplified methods to model the installation process against the full simulation with the Eulerian modelling approach, the importance of modelled soft soil features have been quantified using Design of Experiment (DoE).

The installation methods compared include the Shallow Strain Path Method, the simplified horizontal numerical Cavity Expansion Method and the coupled Eulerian large deformation framework. Modified Cam Clay (MCC) was used as a constitutive model in the methods using the Finite Element Method with an effective-stress based model.

The full pile penetration was modelled in DoE using SCLAY1S. Additional studies on the impact of rate-dependency and small strain stiffness were added in the detailed analyses using Creep-SCLAY1S-ss.

A brief summary of some key results and conclusions is provided in the following:

(i) The influence of the modelled detail of pile installation matters most for the displacements in the soil close to the pile ($< 5R$). At distances beyond this, the difference in the predicted displacements between the horizontally expanded pile and the vertically penetrated pile vanishes.

(ii) The emerging stiffness of the soil governs the mass-displacements which initially occur under constant volume conditions. The elastic stiffness is shown to have a significant influence on the initial distribution of the displaced soil. During dissipation, a reversal of movement occurs due to the compression of the soil close to the pile. The magnitude of consolidation displacements is strongly influenced by the soil features modelled.

(iii) The time for the displacements from consolidation to develop increases with the increased distance from the installed pile. The degree of consolidation, as measured by the excess pore pressures at the pile shaft, is a good approximation for the degree of consolidation movement close to the pile. The time needed for full consolidation is ≈ 10 times longer at a distance of $10R$ compared to the time needed at a distance of $0.5R$.

(iv) The dimensionless relation for the short-term displacements proposed by Sagaseta (2001) holds for the short-term displacements but is not valid in the long-term situation after excess pore water pressures have dissipated.

Paper E: "A simple method for predicting cohesive pile deformations from displacement pile installation induced ground movement"

Paper E relies on a simplified numerical method to predict the cumulative displacements of two existing buildings in Gothenburg, Sweden caused by the installation of a displacement pile in clay. Numerical predictions of the displacements are compared to the field measurements. The numerical predictions are conducted for both a greenfield setting and considering the influence of the existing structures.

A brief summary of some key results and conclusions is provided in the following:

(i) The existing buildings are influencing the soil displacements from nearby pile installation in clay.

(ii) The numerical model is able to predict the general distribution of the displacements in the soils as measured in the field, although the absolute magnitudes are not captured well.

(iii) The greenfield displacements predicted using SSPM and FEM are showing comparable distribution and magnitude of displacements.

Paper F: "Quantifying the response of piled structures from displacements induced by pile installation in soft clay"

This paper investigates the influence of domain size and the presence of an existing building on the displacements in the soil from pile installation in natural clay. The study is conducted using a constant volume linear elastic soil response in combination with a simplified numerical cavity expansion of the pile (group). The influence of the existing structure embedded in the soil is simplified using plate and embedded beam elements.

The influence of the domain size is studied using 3D Finite Element Method and compared to the displacements predicted by the SSPM method. The deformed shape of an existing foundation with properties representative for piled foundations, is studied in detail and used to define a set of response parameters. The response parameters relate the predicted greenfield displacements, such as those that can be calculated with SSPM, to the actual movement and deformations of the existing structures. The response parameters are used in a systematic study on the influence of relative pile length and relative distance between the existing structure and the installed pile. Additionally, the influence of relative stiffness between the soil and the structure, as well as the influence of foundation size and number of piles, are studied.

A brief summary of some key results and conclusions is provided in the following:

(i) The vertical extent of the domain influences the predicted displacements when the piles are installed all the way to the bottom boundary. The effect of the bottom boundary vanishes as the distance between the base of the pile and the boundary increases beyond 0.3 times the length of the installed pile.

(ii) The horizontal extent of the domain strongly influences the distribution of horizontal and vertical displacements, which manifest as increased vertical displacements and reduced horizontal displacements when reducing the domain size. The influence is considerable even at locations that are at a distance larger than one pile length from the boundary. The influence of the domain size on displacements should be considered in all situations, including field conditions, physical model tests, and numerical simulations.

(iii) The study shows that existing piles restrain the vertical displacements while having a limited influence on the magnitude of horizontal displacements.

(iv) A foundation slab restrains and redistributes horizontal displacements without substantially influencing the vertical displacements. The mean greenfield displacement along an existing foundation can serve as a good estimate to the horizontal rigid body movement of the structure.

(v) The restraint caused by the existing foundation can be uniquely linked to the relation between the relative distance between the new and existing pile group L_i/D and the relative length between the existing and new pile $(L_i - L_{ex})/L_i$.

(vi) The deflection ratio and the curvature are strongly linked to the horizontal restraint of the pile head.

6 Conclusions & recommendations

6.1 Conclusions

Urban densification necessitates a system perspective for the design of deep foundations. Prefabricated piles, as commonly used in soft natural clays, lead to mass-displacements and changes in the state of the soil. Therefore, the spatio-temporal response of pile installation into the geotechnical system has been quantified. The focus was on investigating displacement piles installed in soft natural clays over the different stages of the pile cycle.

Modelling pile penetration
Simulations of the penetration of displacement piles into soft natural clay were successfully conducted using an advanced numerical method that combines i) a numerical framework able to handle the large deformations in the soil during pile installation, ii) a hydromechanically coupled effective stress formulation, iii) a set of advanced effective stress-based constitutive models. The numerical method proposed was successfully benchmarked against CPTu penetration over the full range of emerging drainage conditions, by comparing the influence of change in (modelled) soft soil features on the CPTu response.

Additionally, the pile test at the Bothkennar test site was simulated as a first step towards simulating the complete spatio-temporal response of pile installation in the geotechnical system. This included model calibration against laboratory data, simulation of the installation process and the pile load test. The results demonstrate that the proposed method allows for the quantification of the evolving state over the course of the pile cycle in a soft natural clay. The numerical results highlight the interaction between the non-standard soil features of destructuration and rate-dependence in the penetration problem. The installation of the pile leads to destructuration in the clay close to the pile, which results in a significantly changed load-displacement response of the pile upon loading, compared to a wished-in-place pile. This is a strong indication that in case increasingly more complex soil features are included in system-level engineering, the logic behind assuming wished-in-place piles should be revisited.

Mass-displacements in soft natural clay from pile installation
The mass-displacements from pile installation were studied using different numerical prediction methods. The complexity of the models varied with respect to the simplifications made for modelling the mechanism of pile installation and the soil behaviour. The predicted displacements close to the pile were impacted most when comparing (numerical) Cavity Expansion Methods, the Shallow Strain Path Method and the Eulerian Finite Element method. The differences in the predicted displacements between the modelling methods rapidly vanished at distances exceeding $5R$. The stiffness of the soil governs the predicted displacements. In the short-term, all of the prediction methods are displacing the clay under constant volume, either due to assumptions in the method or emerging from the coupled response of the soil-pile system. Therefore, the differences between methods are small at larger distances.

During equalisation, however, the dissipation of the excess pore water pressures from the installation stage softens the system. This softening can only be captured by effective stress-based constitutive models combined with consolidation analysis. The features of the soft natural clay (as simulated with the SCLAY1S model family) strongly impact the magnitude of the displacements in the

soil during consolidation. The time required for the consolidation movement to fully develop varies significantly with the radial distance from the pile. An increase in the distance from the pile leads to an increasing consolidation time. The results of a parametric study also highlighted the importance of stiffness and its gradient in the system for the emerging mass displacements. The latter is further corroborated by the large impact of small-strain stiffness on the predicted short-term displacement response.

Impact of constraints in the domain
The importance of stiffness (gradients) in the geotechnical system was further explored by investigating the influence of existing deep foundations and the domain size on the predicted mass-displacements resulting from pile installation. The findings from the single pile study on required model complexity were exploited to set up a simplified 3D Finite Element Analysis in which pile installation was simulated using numerical cavity expansion and the soil as an elastic material under constant volume conditions.

The results from the simplified 3D FEA show that existing structures significantly redistribute the soil displacements in their stiff direction, *i.e.*, horizontally for a slab on the surface and vertically for the existing pile foundation. The change in the boundary conditions posed by the size of the domain was shown to have a major impact on the predicted displacements. The latter highlights the importance of the geometry of the problem domain, *i.e.*, in the field, numerical analysis or physical model tests, in which the piles are installed.

Final remarks
All factors that influence the magnitude of displacements in soft (natural) clays due to installation of displacement piles can be attributed to basic principles of soil mechanics. In the short term, the stiffness of the system is mainly governed by emerging undrained conditions, and in the long term, by the effective stress properties and evolving state of the soil. Additionally, the stiffness constraints given by the system, *e.g.*, existing foundations and bedrock, influence the distribution of soil displacements. Numerical modelling can be used to distinguish the relative importance of these factors.

6.2 Recommendations

The research has led to the following recommendations for modelling pile installation in natural soft clays:

(i) In absence of complex site-conditions, SSPM remains a valuable tool for estimating the mass-displacement from pile installation in soft natural clays. However, in critical situations, such as, *e.g.*, piling close to existing structures, slopes, excavations and non-linear stiffness profiles, a simplified 3D finite element analysis that accounts for the stiffness distribution in the system is recommended.

(ii) For asset owners, the normalised response charts proposed herein can be used as a first estimate on the potential damage to an existing structure.

(iii) The complexity of the constitutive model used should be balanced by the complexity of the modelling of the pile installation process. Complex models, such as Creep-SCLAY1S, should not be combined with a pile that is wished-in-place in the numerical model.

(iv) Over time, soil displacements from pile installation are partly reversed, and the undrained situation is critical for existing structures. New structures that are constructed after the installed piles, yet before the reversed movement is finished, will be impacted. In an urban setting, such as Gothenburg, with multiple construction activities comprising thousands of piles in the past decade, the past piling activities are still influencing the ongoing soil displacements in the geotechnical system.

The following recommendations should be considered for future research directions:

(i) The temporal evolution of soil displacements due to the installation of multiple piles should be studied further and linked to the degree of consolidation in the system.

(ii) The mesh dependency for strain softening constitutive models in Finite Element Analysis, such as Creep-SCLAY1S, could be reduced by using numerical regularisation using non-local integration schemes for the constitutive model. Recently, non-local methods have been proposed for Large Deformation Finite Element analyses, including ALE remeshing strategies (Singh et al. 2021), Eulerian (Chen et al. 2023) and Coupled Lagrangian Eulerian (Qi et al. 2023) methods. The calibration of the internal length-scales, however, is non-trivial when using standard laboratory data on cylindrical specimens (Romero-Olán et al. 2024)

(iii) Post peak calibration of the constitutive model should be performed on boundary value level which requires non-local laboratory data, such as those obtained from *operando* tests combined with x-ray computed tomography.

(iv) This study focused on modelling the impact of mass displacements from pile installation in natural clays. However, common mitigation measures to reduce the mass-displacement, such as pre-drilling and trenching, also influence the state of the geotechnical system with time. The methods presented in this work are suitable to investigate the latter mitigation measures.

References

Abu-Farsakh, M., Rosti, F., & Souri, A. (2015). Evaluating pile installation and subsequent thixotropic and consolidation effects on setup by numerical simulation for full-scale pile load tests. *Canadian Geotechnical Journal*, *52*(11), 1734–1746. https://doi.org/10.1139/cgj-2014-0470 (cit. on pp. 31, 33, 34).

Allman, M. A., & Atkinson, J. H. (1992). Mechanical properties of reconstituted Bothkennar soil. *Géotechnique*, *42*(2), 289–301. https://doi.org/10.1680/geot.1992.42.2.289 (cit. on p. 13).

Amavasai, A., Sivasithamparam, N., Dijkstra, J., & Karstunen, M. (2018). Consistent Class A & C predictions of the Ballina test embankment. *Computers and Geotechnics*, *93*, 75–86. https://doi.org/10.1016/j.compgeo.2017.05.025 (cit. on p. 14).

Bergdahl, U., & Nilsson, Å. (1974). *Pålning for Silo 68 i Köping En redovisning av mätresultat*. Särtryck och preliminära rapporter nr 44, Ingenjörsvetenskapsakademien, Pålkommisionen. Stockholm. (Cit. on p. 29).

Birmpilis, G., Andò, E., Stamati, O., Hall, S. A., Gerolymatou, E., & Dijkstra, J. (2022). Experimental quantification of 3D deformations in sensitive clay during stress-probing. *Géotechnique*, *73*(8), 655–666. https://doi.org/10.1680/jgeot.21.00114 (cit. on p. 7).

Box, G. E., & Draper, R. D. (2006). *Response Surfaces, Mixtures, and Ridge Analyses, 2nd Edition* (2nd). Wiley & Sons. https://doi.org/10.1002/0470072768 (cit. on p. 51).

Bozkurt, S., Abed, A., & Karstunen, M. (2023). Finite element analysis for a deep excavation in soft clay supported by lime-cement columns. *Computers and Geotechnics*, *162*. https://doi.org/10.1016/j.compgeo.2023.105687 (cit. on p. 14).

Bozozuk, M., Fellenius, B. H., & Samson, L. (1978). Soil disturbance from pile driving in sensitive clay. *Canadian Geotechnical Journal*, *15*, 346–361. https://doi.org/10.1139/t79-048 (cit. on pp. 3, 25, 27).

Brown, M. J., Hyde, A. F. L., & Anderson, W. F. (2006). Analysis of a rapid load test on an instrumented bored pile in clay. *Géotechnique*, *56*(9), 627–638 (cit. on p. 23).

Bui, H. H., Sako, K., & Fukagawa, R. (2007). Numerical simulation of soil-water interaction using smoothed particle hydrodynamics (SPH) method. *Journal of Terramechanics*, *44*, 339–346. https://doi.org/10.1016/j.jterra.2007.10.003 (cit. on p. 33).

Burland, J. (1990). On the compressibility and shear strength of natural clays. *Géotechnique*, *40*(3), 329–378. https://doi.org/10.1680/geot.1990.40.3.329 (cit. on pp. 8, 12).

Castro, J., & Karstunen, M. (2010). Numerical simulations of stone column installation. *Canadian Geotechnical Journal*, *47*(10), 1127–1138. https://doi.org/10.1139/T10-019 (cit. on pp. 14, 32, 34).

Ceccato, F., Beuth, L., Vermeer, P. A., & Simonini, P. (2016). Two-phase Material Point Method applied to the study of cone penetration. *Computers and Geotechnics*, *80*, 440–452. https://doi.org/10.1016/j.compgeo.2016.03.003 (cit. on pp. 4, 33).

Chen, J., Hawlader, B., Roy, K., & Pike, K. (2023). A nonlocal Eulerian-based finite-element approach for strain-softening materials. *Computers and Geotechnics*, *154*. https://doi.org/10.1016/j.compgeo.2022.105114 (cit. on p. 65).

Chen, L. T., & Poulos, H. G. (1997). Piles subjected to lateral soil movements. *Journal of Geotechnical and Geoenvironmental Engineering*, *123*(9), 802–811 (cit. on p. 29).

Chow, Y. K., & Teh, C. I. (1990). A theoretical study of pile heave. *Géotechnique*, *40*(1), 1–14. https://doi.org/10.1680/geot.1990.40.1.1 (cit. on p. 29).

Clayton, C. R. (2011). Stiffness at small strain: Research and practice. *Géotechnique*, *61*(1), 5–37. https://doi.org/10.1680/geot.2011.61.1.5 (cit. on p. 8).

Cooke, R., & Price, G. (1973). Strains and displacements around friction piles. *Proc., 8th Int. Conf. Soil Mech. Found. Engng., Moscow, 3/9*, 53–60. https://doi.org/10.1016/0266-1144(84)90012-8 (cit. on p. 29).

Crosta, G. B., Imposimato, S., & Roddeman, D. G. (2003). Numerical modelling of large landslides stability and runout. *Natural Hazards and Earth System Science*, *3*, 523–538. https://doi.org/10.5194/nhess-3-523-2003 (cit. on p. 35).

Crosta, G. B., Imposimato, S., & Roddeman, D. (2016). Landslide spreading, impulse water waves and modelling of the Vajont rockslide. *Rock Mechanics and Rock Engineering*, *49*, 2413–2436. https://doi.org/10.1007/s00603-015-0769-z (cit. on p. 35).

Cummings, A. E., Kerkhoff, G. O., & Peck, R. B. (1950). Effect of Driving Piles into Soft Clay. *Transactions of the American Society of Civil Engineers*, *115*(1), 275–285. https://doi.org/10.1061/taceat.0006327 (cit. on pp. 8, 25).

Cyril, P. A., Kok, S. T., Song, M. K., Chan, A., Wong, J. Y., & Choong, W. K. (2022). Smooth particle hydrodynamics for the analysis of stresses in soil around Jack-in Pile. *European Journal of Environmental and Civil Engineering*, *26*(1), 94–120. https://doi.org/10.1080/19648189.2019.1649198 (cit. on p. 33).

De Melo, D. L., Dejong, J. T., Kendall, A., & Lehane, B. M. (2024). Life cycle based considerations in design of driven piles in sand. *Proceedings of the Institution of Civil Engineers: Engineering Sustainability*, *177*(6), 389–401. https://doi.org/10.1680/jensu.23.00099 (cit. on p. 3).

DeJong, J. T., & Randolph, M. (2012). Influence of Partial Consolidation during Cone Penetration on Estimated Soil Behavior Type and Pore Pressure Dissipation Measurements. *Journal of Geotechnical and Geoenvironmental Engineering*, *138*(7), 777–788. https://doi.org/10.1061/(asce)gt.1943-5606.0000646 (cit. on pp. 21, 45).

Dijkstra, J., Broere, W., & Heeres, O. M. (2011). Numerical simulation of pile installation. *Computers and Geotechnics*, *38*(5), 612–622. https://doi.org/10.1016/j.compgeo.2011.04.004 (cit. on pp. 4, 33, 35).

Dobry, R., & Vucetic, M. (1987). Dynamic properties and seismic response of soft clay deposits. *In Proc. Int. Symp. on Geotech. Engrg. of Soft Soils Vol. 2*, 51–87 (cit. on p. 8).

Doherty, P., & Gavin, K. (2011). The Shaft Capacity of Displacement Piles in Clay: A State of the Art Review. *Geotechnical and Geological Engineering*, *29*(4), 389–410. https://doi.org/10.1007/s10706-010-9389-2 (cit. on p. 23).

Doherty, P., & Gavin, K. (2013). Pile Aging in Cohesive Soils. *Journal of Geotechnical and Geoenvironmental Engineering*, *139*(9). https://doi.org/10.1061/(ASCE)GT.1943-5606.0000884 (cit. on pp. 12, 24).

Dugan, J. P., & Freed, D. L. (1984). Ground Heave Due to Pile Driving. *International Conference on Case Histories in Geotechnical Engineering,28*, (May) (cit. on pp. 28, 29).

Edstam, T., & Kullingsjö, A. (2010). Ground displacements due to pile driving in Gothenburg clay. *Proceedings of the 7th European Conference on Numerical Methods in Geotechnical Engineering*, 625–630. https://doi.org/10.1201/b10551-114 (cit. on pp. 27, 32, 34).

Fellenius, B. H., & Samson, L. (1976). Testing of drivability of concrete piles and disturbance to sensitive clay. *Canadian Geotechnical Journal*, *13*(2), 139–160 (cit. on p. 25).

Gens, A., & Nova, R. (1993). Conceptual bases for a constitutive model for bonded soils and weak rocks. *Geotech. Engrg. of Hard Soils-Soft Rocks.* (cit. on p. 16).

Gras, J. P., Sivasithamparam, N., Karstunen, M., & Dijkstra, J. (2018). Permissible range of model parameters for natural fine-grained materials. *Acta Geotechnica*, *13*(2), 387–398. https://doi.org/10.1007/s11440-017-0553-1 (cit. on p. 14).

Graham, J., Noonan, M. L., & Lew, K. V. (1983). Yield states and stress-strain relationships in a natural plastic clay. *Canadian Geotechnical Journal*, *20*(3), 502–516. https://doi.org/10.1139/t83-058 (cit. on p. 9).

Gue, S. S. (1984). *Ground Heave Around Driven Piles in Clay* [Doctoral dissertation, University of Oxford]. (Cit. on pp. 27, 28).

Hagerty, D., & Peck, R. (1971). Heave and lateral movements due to pile driving. *Journal of the Soil Mechanics and Foundations Division*, *97*(11), 1513–1532 (cit. on pp. 27–29).

Hamann, T., Qiu, G., & Grabe, J. (2015). Application of a Coupled Eulerian-Lagrangian approach on pile installation problems under partially drained conditions. *Computers and Geotechnics*, *63*, 279–290. https://doi.org/10.1016/j.compgeo.2014.10.006 (cit. on p. 4).

Hauser, L., & Schweiger, H. F. (2021). Numerical study on undrained cone penetration in structured soil using G-PFEM. *Computers and Geotechnics*, *133*, 104061. https://doi.org/10.1016/j.compgeo.2021.104061 (cit. on p. 31).

Hoang, L. T., Dao, K. X., Xiong, X., & Matsumoto, T. (2022). Performance analysis of a jacked-in single pile and pile group in saturated clay ground. *Soils and Foundations*, *62*(1), 101094. https://doi.org/10.1016/j.sandf.2021.101094 (cit. on p. 33).

Hsieh, Y.-M., Dang, P. H., & Lin, H.-D. (2017). How Small Strain Stiffness and Yield Surface Affect Undrained Excavation Predictions. *International Journal of Geomechanics*, *17*(3). https://doi.org/10.1061/(asce)gm.1943-5622.0000753 (cit. on p. 18).

Huetink, H. (1992). *On the simulation of thermo-mechanical forming processes* [Doctoral dissertation, University of Twente]. (Cit. on p. 35).

Hunt, C. E., Pestana, J. M., Bray, J. D., & Riemer, M. (2002). Effect of pile installation on static and dynamic properties of soft clays. *Journal of Geotechnical and Geoenvironmental Engineering*, *128*(1), 13–24. https://doi.org/10.1061/40505(285)15 (cit. on pp. 25, 26).

Isaksson, J., Yannie, J., Karlsson, M., & Dijkstra, J. (2022). Simulation of CPT penetration in sensitive clay. In Gottardi & Tonni (Eds.), *Proceedings of the 5th International Symposium on Cone Penetration Testing, CPT 2022* (pp. 480–485). CRC Press. https://doi.org/10.1201/9781003308829-67 (cit. on p. 77).

Isaksson, J., Karlsson, M., & Dijkstra, J. (2023). Modelling pile installation in soft natural clays. In L. Zdravkovic, S. Kontoe, T. DMG, & T. A. (Eds.), *Proceedings 10th European Conference on Numerical Methods in Geotechnical Engineering*. https://doi.org/10.53243/NUMGE2023-48 (cit. on p. 85).

Isaksson, J., Li, Y., & Hall, L. (2024). A simple method for predicting cohesive pile deformations from displacement pile installation induced ground movement. *19th Nordic Geotechnical Meeting, Gothenburg* (cit. on p. 153).

Isaksson, J., Karlsson, M., & Dijkstra, J. (2025a). Quantifying the response of piled structures from displacements induced by pile installation in soft clay. *Canadian Geotechnical Journal,* [Preprint]. https://doi.org/10.1139/cgj-2024-0387 (cit. on pp. 45, 163).

Isaksson, J., Tahershamsi, H., & Dijkstra, J. (2025b). On modelling pile installation in soft natural clay. *Submitted manuscript* (cit. on p. 125).

Isaksson, J., & Dijkstra, J. (Forthcoming). Modeling the pile cycle of an axially loaded pile in sensitive natural clay. *Journal of Geotechnical and Geoenvironmental Engineering*. https://doi.org/10.1061/JGGEFK/GTENG-13179 (cit. on p. 93).

Karlsrud, K., Jensen, T. G., Lied, E. K. W., Nowacki, F., & Simonsen, A. S. (2014). Significant ageing effects for axially loaded piles in sand and clay verified by new field load tests. *Proceedings of the Offshore Technology Conference*. https://doi.org/10.4043/25197-MS (cit. on p. 24).

Karlsson, M., Emdal, A., & Dijkstra, J. (2016). Consequences of sample disturbance when predicting long-term settlements in soft clay. *Canadian Geotechnical Journal*, *53*(12), 1965–1977. https://doi.org/10.1139/cgj-2016-0129 (cit. on p. 42).

Karstunen, M., & Amavasai, A. (2017). *BEST SOIL: Soft soil modelling and parameter determination*. Chalmers University of Technology, Engineering Geology & Geotechnics. Gothenburg. (Cit. on pp. 42, 44).

Karlsson, M., Yannie, J., & Dijkstra, J. (2019). Modeling Aging of Displacement Piles in Natural Soft Clay. *Journal of Geotechnical and Geoenvironmental Engineering*, *145*(10). https://doi.org/10.1061/(ASCE)GT.1943-5606.0002110 (cit. on pp. 14, 24, 31, 33, 34).

Karlsrud, K., & Haugen, T. (1985). Axial static capacity of steel model piles in overconsolidated clay. *11th International Conference on Soil Mechanics and Foundation Engineering (San Francisco)*, 1401–1406. https://doi.org/10.1016/0266-1144(84)90012-8 (cit. on pp. 25, 26).

Karlsrud, K. (2012). *Prediction of load-displacement behaviour and capacity of axially loaded piles in clay* [Doctoral dissertation, Norwegian University of Science and Technology]. (Cit. on pp. 23, 24).

Karstunen, M. (2023). From theory to practice-numerical modelling of geostructures on soft natural clays. In Zdravkovic L, Kontoe S, Taborda DMG, & Tsiampousi A (Eds.), *Proceedings 10th European Conference on Numerical Methods in Geotechnical Engineering*. https://doi.org/10.53243/NUMGE2023-434 (cit. on p. 3).

Koskinen, M., Karstunen, M., & Wheeler, S. (2002). Modelling destructuration and anisotropy of a natural soft clay. In Mestat (Ed.), *Proceedings 5th European Conference Numerical Methods in Geotechnical Engineering* (pp. 11–19). (Cit. on pp. 12, 14, 15).

Koskinen, M. (2014). *Plastic anisotropy and destructuration of soft Finnish clays* [Doctoral dissertation, Aalto University]. Aalto University. (Cit. on p. 9).

Larsson, R. (1977). *Basic behaviour of Scandinavian soft clays* (No. 4). Statens Geotekniska Institut. Linköping. (Cit. on pp. 9–11).

Lehane, B. M., & Gill, D. (2004). Displacement fields induced by penetrometer installation in an artificial soil. *International Journal of Physical Modelling in Geotechnics*, *4*(1), 25–36. https://doi.org/10.1680/ijpmg.2004.040103 (cit. on p. 27).

Lehane, B. M., O'loughlin, C. D., Gaudin, C., & Randolph, M. F. (2009). Rate effects on penetrometer resistance in kaolin. *Géotechnique*, *59*(1), 41–52. https://doi.org/10.1680/geot.2007.00072 (cit. on p. 21).

Lehane, B. M., Liu, Z., Bittar, E. J., Nadim, F., Lacasse, S., Bozorgzadeh, N., Jardine, R., Ballard, J.-C., Carotenuto, P., Gavin, K., Gilbert, R. B., Bergan-Haavik, J., Jeanjean, P., & Morgan, N. (2022). CPT-Based Axial Capacity Design Method for Driven Piles in Clay. *Journal of Geotechnical and Geoenvironmental Engineering*, *148*(9), 1–18. https://doi.org/10.1061/(asce)gt.1943-5606.0002847 (cit. on pp. 23, 59).

Lehane, B. M., & Jardine, R. J. (1994). Displacement-pile behaviour in a soft marine clay. *Canadian Geotechnical Journal*, *31*(2), 181–191. https://doi.org/10.1139/t94-024 (cit. on p. 59).

Leroueil, S., Tavenas, F., Brucy, F., Rochelle, P. L., & Roy, M. (1979). Behavior of destructured natural clays. *Journal of the geotechnical engineering division*, *105*(6), 759–778 (cit. on p. 12).

Leroueil, S., Kabbaj, M., Tavenas, F., & Bouchard, R. (1985). Stress–strain–strain rate relation for the compressibility of sensitive natural clays. *Géotechnique*, *35*(2), 159–180. https://doi.org/10.1680/geot.1986.36.2.283 (cit. on pp. 10, 11).

Leroueil, S., & Vaughan, P. R. (1990). The general and congruent effects of structure in natural soils and weak rocks. *Géotechnique*, *40*(3), 467–488. https://doi.org/10.1680/geot.1990.40.3.467 (cit. on p. 9).

Leroueil, S. (1996). Compressibility of Clays: Fundamental and Practical Aspects. *Journal of Geotechnical Engineering*, *122*(7), 534–543. https://doi.org/10.1061/(asce)0733-9410(1996)122:7(534) (cit. on p. 12).

Liyanapathirana, D. S. (2009). Arbitrary Lagrangian Eulerian based finite element analysis of cone penetration in soft clay. *Computers and Geotechnics*, *36*(5), 851–860. https://doi.org/10.1016/j.compgeo.2009.01.006 (cit. on pp. 33, 38, 39).

Lu, Q., Randolph, M. F., Hu, Y., & Bugarski, I. C. (2004). A numerical study of cone penetration in clay. *Géotechnique*, *54*(4), 257–267. https://doi.org/10.1680/geot.2004.54.4.257 (cit. on pp. 4, 33).

Mahmoodzadeh, H., & Randolph, M. F. (2014). Penetrometer Testing: Effect of Partial Consolidation on Subsequent Dissipation Response. *Journal of Geotechnical and Geoenvironmental Engineering*, *140*(6), 04014022. https://doi.org/10.1061/(asce)gt.1943-5606.0001114 (cit. on p. 45).

Massarsch, K. R. (1976). *Soil movements caused by pile driving in clay* [Doctoral dissertation, Kungliga Tekniska Högskolan]. (Cit. on pp. 28, 29).

Mayne, P. W., & Kulhawy, F. H. (1982). K 0-0CR RELATIONSHIPS IN SOIL. *Journal of the Geotechnical Engineering Division*, *108*(8), 851–872 (cit. on p. 9).

Mitchell, J., & Soga, K. (2005). *Fundamentals of Soil Behavior* (3rd ed.). John Wiley & Sons, Inc. (Cit. on pp. 8, 9, 12).

Monforte, L., Arroyo, M., Carbonell, J. M., & Gens, A. (2018). Coupled effective stress analysis of insertion problems in geotechnics with the Particle Finite Element Method. *Computers and Geotechnics*, *101*(February), 114–129. https://doi.org/10.1016/j.compgeo.2018.04.002 (cit. on p. 4).

Monforte, L., Gens, A., Arroyo, M., Mánica, M., & Carbonell, J. M. (2021). Analysis of cone penetration in brittle liquefiable soils. *Computers and Geotechnics*, *134*(104123). https://doi.org/10.1016/j.compgeo.2021.104123 (cit. on pp. 31, 33, 34).

Ni, Q., Hird, C. C., & Guymer, I. (2010). Physical modelling of pile penetration in clay using transparent soil and particle image velocimetry. *Géotechnique*, *60*(2), 121–132. https://doi.org/10.1680/geot.8.P.052 (cit. on pp. 3, 27, 40, 41).

Orrje, O., & Broms, B. (1967). Effects of pile driving on soil properties. *Journal of the Soil Mechanics and Foundation Divisions*, *93*(5), 59–73 (cit. on p. 27).

Ottolini, M., Dijkstra, J., & van Tol, F. (2014). Immediate and long-term installation effects adjacent to an open-ended pile in a layered clay. *Canadian Geotechnical Journal*, *52*(7), 982–991. https://doi.org/10.1139/cgj-2014-0222 (cit. on pp. 25, 27).

Pålkommissionen. (2024). *Pålstatistik för Sverige 2023*. (Cit. on p. 3).

Pestana, J. M., Hunt, C. E., & Bray, J. D. (2002). soil deformation and excess pore pressure field around a closed-ended pile. *Journal of Geotechnical and Geoenvironmental Engineering*, *128*(1), 669–671. https://doi.org/10.1061/(ASCE)1090-0241(2003)129:7(669) (cit. on p. 29).

Phek, J., Tan, S., Goh, S. H., & Tan, S. A. (2023). Numerical Analysis of a Jacked-In Pile Installation in Clay. *23*(6), 1–14. https://doi.org/10.1061/IJGNAI.GMENG-7946 (cit. on pp. 4, 31, 33, 34).

Phoon, K. K., & Kulhawy, F. H. (1999). Characterization of geotechnical variability. *Canadian Geotechnical Journal*, *36*(4), 612–624. https://doi.org/10.1139/t99-038 (cit. on p. 51).

Qi, Y., Bransby, F., & O'Loughlin, C. D. (2023). Strain regularisation using a non-local method in Coupled Eulerian-Lagrangian analyses. *Computers and Geotechnics*, *164*. https://doi.org/10.1016/j.compgeo.2023.105826 (cit. on p. 65).

Randolph, M. F., & Gourvenec, S. (2011). *Offshore Geotechnical Engineering*. CRC Press. https://doi.org/10.1201/9781315272474 (cit. on pp. 5, 55).

Randolph, M. F., Carter, J. P., & Wroth, C. P. (1979). Driven Piles in clay—The Effects of Installation and Subsequent Consolidation. *Géotechnique*, *29*(4), 361–393. https://doi.org/10.1680/geot.1979.29.4.361 (cit. on p. 33).

Randolph, M. F. (2003). Science and empiricism in pile foundation design. *Geotechnique*, *53*(10), 847–875. https://doi.org/10.1680/geot.2003.53.10.847 (cit. on p. 23).

Rehkopf, J. C. (2001). *Predictions and measurements of ground movements due to pile driving in clay* [Doctoral dissertation, Massachusetts Institute of Technology]. (Cit. on p. 27).

Ren, Y., Yang, S., Andersen, K. H., Yang, Q., & Wang, Y. (2021). Thixotropy of soft clay: A review. *Engineering Geology*, *287*(2), 106097. https://doi.org/10.1016/j.enggeo.2021.106097 (cit. on p. 31).

Robertson, P. K. (1990). Soil classification using the cone penetration test. *Canadian Geotechnical Journal*, *27*(1), 151–158. https://doi.org/10.1139/t90-014 (cit. on p. 38).

Roddeman, D. (2024). Tochnog Professional User's manual. (Cit. on pp. 35, 44).

Romero-Olán, T., Mánica, M. A., Ovando-Shelley, E., Rodríguez-Rebolledo, J. F., & Buritica, J. A. (2024). On the Determination of Softening Parameters for Nonlocal Constitutive Models. *Journal of Geotechnical and Geoenvironmental Engineering*, *150*(12). https://doi.org/10.1061/JGGEFK.GTENG-12489 (cit. on p. 65).

Roscoe, K. H., Schofield, A. N., & Wroth, C. P. (1958). On the yielding of soils. *Géotechnique*, *8*(1), 22–53. https://doi.org/10.1680/geot.1958.8.1.22 (cit. on pp. 13, 14).

Roscoe, K., & Burland, J. (1968). On the generalized stress-strain behavior of "wet" clay. In J. Heyman & F. A. Leckie (Eds.), *Engineering Plasticity* (pp. 535–609). Cambridge University Pres. https://doi.org/10.1016/0022-4898(70)90160-6 (cit. on p. 14).

Roy, M., Blanchet, R., Tavenas, F., & Larochelle, P. (1981). Behaviour of a sensitive clay during pile driving. *Canadian Geotechnical Journal*, *18*(1), 67–85. https://doi.org/10.1139/t81-007 (cit. on pp. 25, 26).

Sagaseta, C., Whittle, A. J., & Santagata, M. (1997). Deformation analysis of shallow penetration in clay. *International Journal for Numerical and Analytical Methods in Geomechanics*, *21*(10), 687–719. https://doi.org/10.1002/(SICI)1096-9853(199710)21:10<687::AID-NAG897>3.0.CO;2-3 (cit. on pp. 4, 27).

Sagaseta, W., C. (2001). Prediction of ground movements due to pile driving in clay. *Journal of Geotechnical and Geoenvironmental Engineering*, *127*(1), 55–66. https://doi.org/https://doi.org/10.1061/(ASCE)1090-0241(2001)127:1(55) (cit. on pp. 27, 28, 60).

Sällfors, G. (1975). *Preconsolidation pressure of soft, high-plastic clays* [Doctoral dissertation, Chalmers University of Technology]. (Cit. on pp. 9–11).

Schneider, J. A., Lehane, B. M., & Schnaid, F. (2007). Velocity effects on Piezocone measurements in normally and over consolidated clays. *International Journal of Physical Modelling in Geotechnics*, *7*(2), 23–34. https://doi.org/10.1680/ijpmg.2007.070202 (cit. on pp. 20, 21, 45).

Schneider, J. A., Randolph, M. F., Mayne, P. W., & Ramsey, N. R. (2008). Analysis of Factors Influencing Soil Classification Using Normalized Piezocone Tip Resistance and Pore Pressure Parameters. *Journal of Geotechnical and Geoenvironmental Engineering*, *134*(11), 1569–1586. https://doi.org/10.1061/(asce)1090-0241(2008)134:11(1569) (cit. on p. 38).

Seed, H. B., & Reese, L. C. (1957). The action of soft clay along friction piles. *Transactions of the American Society of Civil Engineers*, *122*(1), 731–754 (cit. on p. 25).

Sellin, C., & Karstunen, M. (2023). Slope stability assessment in sensitive clay with an advanced constitutive model. In L. Zdravkovic, S. Kontoe, D. Taborda, & A. Tsiampous (Eds.), *Proceedings 10th European Conference on Numerical Methods in Geotechnical Engineering* (p. 2023). https://doi.org/10.53243/NUMGE2023-298 (cit. on p. 14).

Sheng, D., Sloan, S. W., & Yu, H. S. (2000). Aspects of finite element implementation of critical state models. *Computational Mechanics*, *26*(2), 185–196. https://doi.org/10.1007/s004660000166 (cit. on p. 15).

Sheil, B. B., McCabe, B. A., Hunt, C. E., & Pestana, J. M. (2015). A practical approach for the consideration of single pile and pile group installation effects in clay: Numerical modelling. *Journal of Geo-Engineering Sciences*, *2*(3,4), 119–142. https://doi.org/10.3233/jgs-140027 (cit. on pp. 32–34).

Singh, V., Stanier, S., Bienen, B., & Randolph, M. F. (2021). Modelling the behaviour of sensitive clays experiencing large deformations using non-local regularisation techniques. *Computers and Geotechnics*, *133*(February), 104025. https://doi.org/10.1016/j.compgeo.2021.104025 (cit. on pp. 4, 65).

Singh, V., Stanier, S., Bienen, B., & Randolph, M. F. (2022). A viscoplastic recoverable sensitivity model for fine-grained soils. *Computers and Geotechnics*, *147*(July). https://doi.org/10.1016/j.compgeo.2022.104725 (cit. on pp. 31, 34).

Sivasithamparam, N., Engin, H. K., & Castro, J. (2015a). Numerical modelling of pile jacking in a soft clay. In Oka, Murukami, Uzuoka, & Kimoto (Eds.), *Proceedings of the 14th International Conference of International Association for Computer Methods and Recent Advances in Geomechanics, 2014*. Taylor & Francis, London. (Cit. on pp. 31, 34).

Sivasithamparam, N., Karstunen, M., & Bonnier, P. (2015b). Modelling creep behaviour of anisotropic soft soils. *Computers and Geotechnics*, *69*, 46–57. https://doi.org/10.1016/j.compgeo.2015.04.015 (cit. on pp. 14, 15).

Sivasithamparam, N., & Castro, J. (2020). Undrained cylindrical cavity expansion in clays with fabric anisotropy and structure: Theoretical solution. *Computers and Geotechnics*, *120*(May 2019), 103386. https://doi.org/10.1016/j.compgeo.2019.103386 (cit. on p. 33).

Sivasithamparam, N., D'Ignazio, M., Tsegaye, A. B., Castro, J., & Madshus, C. (2021). Small strain stiffness within logarithmic contractancy model for structured anisotropic clay. *IOP Conference Series: Earth and Environmental Science*, *710*, 012042. https://doi.org/10.1088/1755-1315/710/1/012042 (cit. on p. 17).

Staubach, P., Tschirschky, L., Machaček, J., & Wichtmann, T. (2023). Monopile installation in clay and subsequent response to millions of lateral load cycles. *Computers and Geotechnics*,

155(July 2022), 105221. https://doi.org/10.1016/j.compgeo.2022.105221 (cit. on pp. 4, 31, 33, 34).

Šuklje, L. (1957). The Analysis of the Consolidation Process by the Isotaches Method. *4th International Conference on Soil Mechanics and Foundation Engineering*, 200–206 (cit. on p. 18).

Tahershamsi, H., & Dijkstra, J. (2022). Using experimental design to assess rate-dependent numerical models. *Soils and Foundations*, *62*(6). https://doi.org/10.1016/j.sandf.2022.101244 (cit. on p. 51).

Tahershamsi, H., Ahmadi Naghadeh, R., Zuada Coelho, B., & Dijkstra, J. (2023). Low amplitude strain accumulation model for natural soft clays below railways. *Transportation Geotechnics*, *42*. https://doi.org/10.1016/j.trgeo.2023.101011 (cit. on pp. 14, 17, 18, 42, 44).

Tavenas, F., Leroueil, S., Rochelle, P. L., & Roy, D. M. (1978). Creep behaviour of an undisturbed lightly overconsolidated clay. *Canadian Geotechnical Journal*, *15*(3), 402–423. https://doi.org/10.1139/t78-037 (cit. on p. 10).

Teh, C. I., & Houlsby, G. (1991). An analytical study of the cone penetration test in clay. *Géotechnique*, *41*(1), 17–34. https://doi.org/10.1680/geot.1992.42.3.529 (cit. on pp. 21, 22).

Tornborg, J., Karlsson, M., Kullingsjö, A., & Karstunen, M. (2021). Modelling the construction and long-term response of Göta Tunnel. *Computers and Geotechnics*, *134*. https://doi.org/10.1016/j.compgeo.2021.104027 (cit. on p. 14).

Tornborg, J., Karlsson, M., & Karstunen, M. (2023). Permanent Sheet Pile Wall in Soft Sensitive Clay. *Journal of Geotechnical and Geoenvironmental Engineering*, *149*(6), 05023003. https://doi.org/10.1061/jggefk.gteng-10955 (cit. on p. 14).

Torstensson, B. (1973). The behaviour of a cohesion pile group in soft clay. *8th International Conference on Soil Mechanics and Foundation Engineering (Moscow)* (cit. on p. 25).

Turkel, B., Orozco-Herrera, J. E., Arboleda-Monsalve, L. G., Nam, B. H., & Jones, L. (2023). Semiempirical Model of Vibration-Induced Ground Deformations due to Impact Pile Driving. *Journal of Geotechnical and Geoenvironmental Engineering*, *149*(11), 04023110. https://doi.org/10.1061/jggefk.gteng-11638 (cit. on p. 29).

van den Berg, P., Borst, R. D., & Huetink, H. (1996). An eulerean finite element model for penetration in layered soil. *International Journal for Numerical and Anaylytical Methods in Geomechanics*, *20*(January 1995), 865–886 (cit. on p. 4).

Vermeer, P. A., & Verruijt, A. (1981). An accuracy condition for consolidation by finite elements. *International Journal for Numerical and Analytical Methods in Geomechanics*, *5*, 1–14 (cit. on p. 45).

Wheeler, S. J., Näätänen, A., Karstunen, M., & Lojander, M. (2003). An anisotropic elastoplastic model for soft clays. *Canadian Geotechnical Journal*, *40*(2), 403–418. https://doi.org/10.1139/t02-119 (cit. on pp. 9, 14).

Wood, D. (1990). *Soil behaviour and critical state soil mechanics*. Cambrigde University Press. (Cit. on p. 14).

Xu, K. J., & Poulos, H. G. (2001). 3-D elastic analysis of vertical piles subjected to "passive" loadings. *Computers and Geotechnics*, *28*, 349–375. https://doi.org/10.1016/S0266-352X(00)00024-0 (cit. on p. 29).

Xu, X., Liu, H., & Lehane, B. M. (2006). Pipe pile installation effects in soft clay. *Proceedings of the Institution of Civil Engineers: Geotechnical Engineering*, *159*(4), 285–296. https://doi.org/10.1680/geng.2006.159.4.285 (cit. on p. 27).

Yi, J. T., Liu, F., Zhang, T. B., Yao, K., & Zhen, G. (2021). A large deformation finite element investigation of pile group installations with consideration of intervening consolidation. *Applied Ocean Research*, *112*(April), 102698. https://doi.org/10.1016/j.apor.2021.102698 (cit. on p. 33).

Zdravković, L., Potts, D. M., & Taborda, D. M. (2021). Integrating laboratory and field testing into advanced geotechnical design. *Geomechanics for Energy and the Environment*, *27*. https://doi.org/10.1016/j.gete.2020.100216 (cit. on p. 3).

Zhou, H., & Randolph, M. F. (2009). Resistance of full-flow penetrometers in rate-dependent and strain-softening clay. *Geotechnique*, *59*(2), 79–86. https://doi.org/10.1680/geot.2007.00164 (cit. on p. 31).

Zhou, H., Liu, H., Randolph, M. F., Kong, G., & Cao, Z. (2017). Experimental and analytical study of X-Section Cast-In-Place concrete pile installation effect. *International Journal of Physical Modelling in Geotechnics*, *17*(2), 103–121. https://doi.org/10.1680/jphmg.15.00037 (cit. on p. 27).

Zhou, P., Li, J., Li, L., & Xie, F. (2021). Analysis of the existing pile response induced by adjacent pile driving in undrained clay. *Computers and Geotechnics*, *138*(June), 104319. https://doi.org/10.1016/j.compgeo.2021.104319 (cit. on p. 29).